https://doi.org/10.1093/plphys/kiad162 PLANT PHYSIOLOGY 2023: 192: 1080–1098

Plant Physiology®

Research Article

Tomato sucrose transporter SlSUT4 participates in flowering regulation by modulating gibberellin biosynthesis

Yufei Liang,[1] Jiayu Bai,[1] Zhilong Xie,[1] Zhaoyuan Lian,[2] Jia Guo,[1] Feiyang Zhao,[3] Yan Liang,[1] Heqiang Huo[2] and Haijun Gong[1,*]

1 Shaanxi Engineering Research Center for Vegetables/College of Horticulture, Northwest A&F University, Yangling, Shaanxi 712100, China
2 Mid-Florida Research and Education Center, University of Florida, Institute of Food and Agricultural Sciences, 2725 South Binion Road, Apopka, FL 32703, USA
3 College of Life Sciences, Northwest A&F University, Yangling, Shaanxi 712100, China

*Author for correspondence: gongnavy@163.com
The author responsible for distribution of materials integral to the findings presented in this article in accordance with the policy described in the Instructions for Authors (https://academic.oup.com/plphys/pages/General-Instructions) is Haijun Gong (gongnavy@163.com).

Abstract

The functions of sucrose transporters (SUTs) differ among family members. The physiological function of SUT1 has been studied intensively, while that of SUT4 in various plant species including tomato (*Solanum lycopersicum*) is less well-understood. In this study, we characterized the function of tomato *SlSUT4* in the regulation of flowering using a combination of molecular and physiological analyses. SlSUT4 displayed transport activity for sucrose when expressed in yeast (*Saccharomyces cerevisiae*), and it localized at both the plasma membrane and tonoplast. SlSUT4 interacted with SlSUT1, causing partial internalization of the latter, the main phloem loader of sucrose in tomato. Silencing of *SlSUT4* promoted SlSUT1 localization to the plasma membrane, contributing to increased sucrose export and thus increased sucrose level in the shoot apex, which promoted flowering. Both silencing of *SlSUT4* and spraying with sucrose suppressed gibberellin biosynthesis through repression of *ent-kaurene oxidase* and *gibberellin 20-oxidase-1* (2 genes encoding key enzymes in gibberellin biosynthesis) expression by SlMYB76, which directly bound to their promoters. Silencing of *SlMYB76* promoted gibberellin biosynthesis. Our results suggest that SlSUT4 is a functional SUT in tomato; downregulation of *SlSUT4* expression enhances sucrose transport to the shoot apex, which promotes flowering by inhibiting gibberellin biosynthesis.

Introduction

Appropriate flowering time is critical for the successful reproduction of plants. Flowering is regulated by both environmental and endogenous factors. The genetic pathways of flowering have been extensively characterized, especially in the model plant Arabidopsis (*Arabidopsis thaliana*), and these mainly include the vernalization, photoperiod, autonomous, gibberellin (GA), thermosensory, and aging pathways (Quiroz et al. 2021). In recent years, researchers have identified more flowering pathways, such as the sugar, stress, and other hormonal signals (Izawa 2021). However, the crosstalk among some of these pathways is still poorly understood.

Sugars are produced from photosynthesis, with sucrose being the primary product (Ding et al. 2019). Sucrose not only serves as a carbon and energy source but also plays a signaling role during plant growth and development (Yoon et al. 2021). Once produced, sucrose is transiently stored in vacuoles of source organs, and it is also transported from source to sink organs via the phloem (Yoon et al. 2021). The long-distance source-sink transport includes 3 steps: (i) sucrose efflux into the apoplasm from the cytosol via Sugar

Received October 27, 2022. Accepted February 26, 2023. Advance access publication March 21, 2023

Will Eventually be Exported Transporters (SWEETs) (Chen et al. 2012); (ii) sucrose uptake from the apoplast into the sieve element–companion cell complex of the phloem, which is mediated by sucrose transporters (SUTs); and (iii) sucrose release from the phloem into sink cells, which is mediated by plasmodesmata or SUTs (Oner-Sieben et al. 2015). Therefore, SUTs play an important role in photoassimilate source-sink partitioning.

SUTs are transmembrane proteins belonging to the major facilitator superfamily, and they are divided into 3 groups (types I, II, and III) according to phylogenetic analysis (Reinders et al. 2012). Type I SUTs only exist in eudicots, and they are essential for some functions, such as phloem loading (Riesmeier et al. 1994) and pollen germination (Sivitz et al. 2008). Type II SUTs can be further separated into 2 subgroups: dicot-specific type IIA and monocot-specific type IIB. Monocot species have been found to use type II SUTs for phloem loading (Aoki et al. 2004; Sivitz et al. 2005; Slewinski et al. 2009). Some type IIB SUTs are involved in phloem unloading and sucrose import into sink tissues (Kühn and Grof 2010). Type III SUTs exist in all land plants, and they are localized at the tonoplast or plasma membrane or both of them (Chincinska et al. 2013, and references therein). Tonoplast-localized SUTs function in sucrose transport from the vacuole into the cytoplasm (Reinders et al. 2008), and plasma membrane-localized ones may be involved in signaling process (Chincinska et al. 2013).

SUTs are encoded by a gene family, which is usually composed of 3 to 9 members (Xu et al. 2018). In tomato (*Solanum lycopersicum*), there are 3 *SUTs - SlSUT1* (Solyc11g017010.1.1), *SlSUT2* (Solyc05g007190.2.1), and *SlSUT4* (Solyc04g076960.2.1), which belong to type I, IIA, and III SUTs, respectively (Reinders et al. 2012). These SUTs are all localized in the enucleate sieve elements of tomato (Reinders et al. 2002). Using the yeast (*Saccharomyces cerevisiae*) two-hybrid split ubiquitin system, Reinders et al. (2002) found that all the 3 SlSUTs have a potential to interact with each other. The function of SlSUT1 in phloem loading and long-distance transport has been verified by antisense inhibition: downregulation of the *SlSUT1* expression brought about inefficient phloem loading, causing delayed development of sink organs (Hackel et al. 2006). SlSUT2 has been proposed as a putative receptor of extracellular sucrose (Barker et al. 2000) and plays a role in pollen tube growth (Hackel et al. 2006). SlSUT2 also interacts with brassinosteroid to affect *arbuscular mycorrhiza* formation (Bitterlich et al. 2014). Relatively, the functional characteristics of *SlSUT4* are less understood. Weise et al. (2000) found that *SlSUT4* was predominantly expressed in sink leaves, stems, cotyledons, and immature fruits. They also observed that SlSUT4 was not functional in sucrose transport when expressed in yeasts and it was localized at the plasma membrane. However, the subcellular localization of SlSUT4 still needs to be confirmed, as differential results have been reported in different plants and even in the same species (Chincinska et al. 2013). For instance, in the *Solanaceous* plant potato (*Solanum tuberosum*), Chincinska et al. (2013) observed a dual localization of StSUT4, i.e. at plasma membrane and most possibly tonoplast as well. Therefore, the functional characteristics of *SlSUT4* still remain to be investigated.

The inductive effect of sucrose on flowering has been observed in different species (Cho et al. 2018; Quiroz et al. 2021). For instance, sucrose levels in the phloem and shoot apex are usually increased at the early stage of flowering process (Pryke and Bernier 1978; Houssa et al. 1991). Sucrose addition generally enhances flowering in different plants, such as oilseed rape (*Brassica campestris*) (Friend et al. 1984), tobacco (*Nicotiana tabacum*) (Teichmanová et al. 2007), Arabidopsis (Yang et al. 2013) and chrysanthemum (*Chrysanthemum morifolium* "Floral Yuuka") with a night break (Sun et al. 2017). Increasing endogenous sucrose levels through transgenic approach also promotes flowering. For example, inhibition of *AGPase* expression in potato leads to an accumulation of soluble sugars including sucrose and glucose in the leaves and earlier flowering (Muller-Rober et al. 1992). In tomato, expressing maize (*Zea mays*) sucrose phosphate synthase gene enhances sucrose accumulation in the leaves, and the plants flower earlier in CO_2-elevated conditions (Micallef et al. 1995). In addition, as mentioned above, SUTs play a key role in sucrose source-sink partitioning. Therefore, modulating the expression of *SUTs* may alter the shoot apex sucrose level and thus flowering time, as observed in potato, where downregulation of the plasma membrane-localized *StSUT4* leads to early flowering and tuberization (Chincinska et al. 2008). Although much evidence has demonstrated the role of sucrose in promoting flowering, the underlying molecular mechanism is still not well-clarified.

GA signaling is one of the early identified genetic pathways of flowering. In plants, the major bioactive GAs include GA_1, GA_3, GA_4, and GA_7 (Yamaguchi 2008). Three classes of enzymes are required for GA biosynthesis from geranylgeranyl diphosphate, i.e. terpene synthases (TPSs), cytochrome P450 monooxygenases (P450s), and 2-oxoglutarate-dependent dioxygenases (Yamaguchi 2008). Two TPSs, *ent*-copalyl diphosphate synthase (CPS) and *ent*-kaurene synthase (KS), catalyze the conversion of geranylgeranyl diphosphate to *ent*-kaurene, which is then converted to GA_{12} by two P450s, *ent*-kaurene oxidase (KO) and *ent*-kaurenoic acid oxidase (KAO) (Yamaguchi 2008). GA 20-oxidase (GA20ox) and GA 3-oxidase (GA3ox) catalyze the production of different bioactive GAs from GA_{12} (Yamaguchi 2008). The role of GA in regulating flowering differs with plant species. For instance, GA promotes flowering in Arabidopsis (Fukazawa et al. 2021), whereas it inhibits flowering in tomato (García-Hurtado et al. 2012; Silva et al. 2019) and apple (*Malus domestica*) (Zhang et al. 2016). In the GA signaling, the binding of GA with its receptor GIBBERELLIN INSENSITIVE DWARF1 (GID1) induces a conformational change of GID1, which creates a surface for binding DELLAs (Willige et al. 2007; Murase et al. 2008). The formation of GA–GID1–DELLA complex stimulates the binding of E3 ubiquitin ligase to DELLAs, resulting in DELLA

degradation (Silverstone et al. 2001) and thus affecting the expression of its target genes, such as those related to flowering (Bao et al. 2020). Therefore, DELLAs play a key role in flowering regulation in the GA signaling pathway.

Accumulating evidence has demonstrated that sucrose signal interplays with the hormonal network, including GA signaling (Sakr et al. 2018; Garg and Kühn 2022). In Arabidopsis, physiological evidence indicates that sucrose-induced anthocyanin biosynthesis is inhibited by exogenous GA (Loreti et al. 2008). Further evidence has demonstrated that sucrose stabilizes DELLA proteins, which act as a positive regulator of anthocyanin biosynthesis (Li et al. 2014). These studies suggest that GA signaling is involved in sucrose signaling pathway in anthocyanin biosynthesis. However, more work is still needed to understand the roles of sucrose signaling in various physiological processes, such as flowering.

In this study, we provide evidence demonstrating that SlSUT4 is a functional SUT in tomato. We also found that downregulation of *SlSUT4* expression via RNA interference (RNAi) enhances sucrose transport to the shoot apex, which promotes tomato flowering by inhibiting GA biosynthesis. The study may help us understand the function of *SlSUT4* and the molecular mechanism of sucrose in promoting flowering.

Results

SlSUT4 cloning and transport activity of SlSUT4

Based on the CDS of *SlSUT4* in "Heinz 1706" (Solyc04g076960.2.1), we cloned this gene from the genotype "M82" by polymerase chain reaction (PCR). The CDS of *SlSUT4* is 1,503-bp-long, which encodes a protein with 500 amino acids (Supplemental Fig. S1, A and B). The CDSs of "M82" and "Heinz 1706" demonstrated base variations at 3 positions (Supplemental Fig. S1A), whereas their protein sequences showed 1 amino acid residue difference at the 480 position (Supplemental Fig. S1B). We also compared the sequences in "M82" with those in "UC82b" and observed 1 base difference, resulting in 1 amino acid residual variation at the 203 position (Supplemental Fig. S1B).

To determine whether SlSUT4 has sucrose transport activity, we expressed the gene in two yeast strains. The results showed that the SUSY7/ura3 yeast cells (a mutant that cannot synthesize invertase; Riesmeier et al. 1992) expressing *SlSUT4*, *AtSUC2*, or *AtSUT4* grew better than the negative control when sucrose was used as the sole carbon source, while their growth did not differ when glucose was provided (Fig. 1, A and B). Esculin is a sucrose analog and has been used for transport activity assay of SUTs (Gora et al. 2012; Garg et al. 2022). In this study, SEY6210 yeast cells expressing *SlSUT4*, *AtSUC2*, or *AtSUT4* took up more esculin than the negative control (empty vector), and the optimum pH for the uptake differed between these SUTs: between 3 and 4 for AtSUC2, and between 4 and 5 for AtSUT4 and SlSUT4 (Fig. 1, C to E). The yeast cells expressing *AtSUC2* demonstrated esculin uptake at different concentrations (0.01 to 8 mM), whereas those expressing *AtSUT4* and *SlSUT4* showed obvious esculin uptake when the substrate concentration was 1 mM or higher (Fig. 1, F to H), suggesting that SlSUT4 and AtSUT4 had a lower affinity to esculin than AtSUC2. These results indicate that similar to AtSUC2 (Sauer and Stolz 1994) and AtSUT4 (Weise et al. 2000), SlSUT4 is a functional SUT.

Subcellular localization of SlSUT4

To investigate the subcellular localization of SlSUT4, the *GFP* gene was fused to *SlSUT4* and transiently expressed in *Nicotiana benthamiana* epidermal cells. The GFP fluorescence signal was generally weak when it was fused to the C-terminus of SlSUT4, while the signal was clear when GFP was fused to the N-terminus (Supplemental Fig. S2, A and B). Therefore, the *GFP-SlSUT4* construct was used for localization analysis by co-expression with a tonoplast marker Atγ-TIP-mCherry and a plasma membrane marker myr-mCherry. The results showed that the GFP signal overlapped with mCherry signal at both plasma membrane and tonoplast (Fig. 2), indicating that SlSUT4 is a tonoplast- and plasma membrane-localized SUT.

SlSUT4-RNAi plants show early flowering

To further investigate the function of *SlSUT4*, we generated *SlSUT4*-overexpressing and RNAi silencing tomato lines (Fig. 3B). The RNAi lines demonstrated earlier flowering phenotype and had fewer leaves at the first floral bud appearance compared with the wild type (Fig. 3, A, C, and D). The tomato *FALSIFLORA* (*FA*) and *MACROCALYX* (*MC*) are the orthologs of *LEAFY* and *APETALA1* in Arabidopsis, respectively, both of which are essential for floral meristem identity (Molinero-Rosales et al. 1999; Silva et al. 2019; Bao et al. 2020). The expression of *FA* and *MC* in *SlSUT4*-RNAi plants was significantly increased (Fig. 3, E and F). However, the expression of two floral integrator genes, *SUPPRESSOR OF OVEREXPRESSION OF CONSTANS 1* (*SOC1*) or *SINGLE FLOWER TRUSS* (*SFT*, an ortholog of *FLOWERING LOCUS T*; Lifschitz et al. 2006; Bao et al. 2020), was not affected by *SlSUT4* silencing (Fig. 3, G and H). To our surprise, the flowering time was not affected by *SlSUT4* overexpression (Fig. 3, A, C, and D), nor was the expression of flowering-related genes (Fig. 3, E to H).

Silencing *SlSUT4* promotes sucrose efflux and increases soluble sugar accumulation in the shoot apex

To examine whether there was any change in the sucrose level between the *SlSUT4*-RNAi and wild-type plants, we analyzed the sucrose concentration in mature (source) leaves at different time of the day. At 10:00 AM (3 h under light), there was no difference in the sucrose concentration between *SlSUT4*-RNAi and wild-type plants (Supplemental Fig. S3A); whereas at 3:00 PM (8 h under light) and 9:00 PM (2 h in dark), *SlSUT4*-RNAi plants had higher sucrose concentration than the wild type

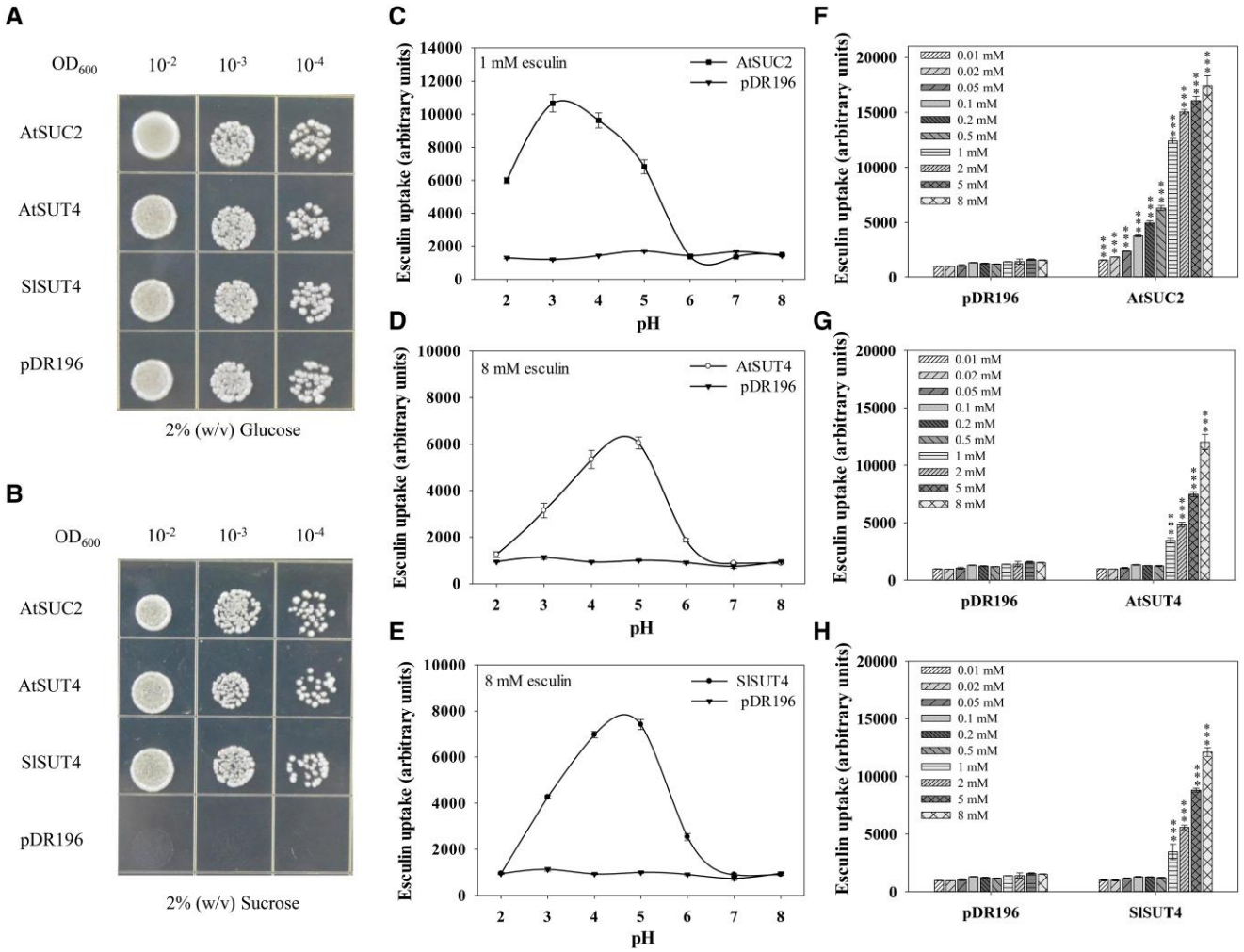

Figure 1. Transport activity of SlSUT4 in yeasts. **A, B)** Growth of sucrose uptake-deficient yeast strain SUSY7/ura3-expressing *SlSUT4* with glucose **(A)** or sucrose **(B)** as the sole carbon source. **C** to **E)** The pH dependence for SUTs to uptake esculin. The transformed SEY6210 yeasts were incubated in 25 mM sodium phosphate buffer (pH 2 to 8) containing 1 or 8 mM esculin for 1 h, and the esculin fluorescence intensity was quantified with a multifunctional enzyme labeling instrument at excitation and emission wavelengths of 367 and 454 nm, respectively. **F** to **H)** Esculin uptake by SEY6210 yeasts expressing *SUTs* at different esculin concentrations. The transformed yeasts were incubated in 25 mM sodium phosphate buffer (pH 4) containing different esculin concentrations for 1 h, and the esculin fluorescence intensity was quantified. Data are means ± SD ($n = 3$). At each esculin concentration, the uptake was compared between SlSUT4 and the empty vector using Student's *t*-test. Asterisks above bars indicate significant differences compared with the empty vector at the corresponding esculin concentrations. ***$P < 0.001$. In both growth and esculin uptake experiments, the yeasts transformed with *AtSUC2* and *AtSUT4* were used as positive controls and empty vector pDR196 as the negative control.

(Supplemental Fig. S3A). In addition, silencing *SlSUT4* did not change the starch concentration in leaves (Supplemental Fig. S3B). In the shoot apex (a sink tissue), the concentrations of sucrose as well as glucose and fructose in the *SlSUT4*-RNAi plants were significantly increased at night (Fig. 4, A to C), which were consistent with the change of sucrose concentrations in source leaves. However, overexpression of *SlSUT4* did not alter the soluble sugar concentrations in the shoot apex (Fig. 4, A to C). Moreover, the sucrose export rate was significantly increased in the *SlSUT4*-RNAi plants (Fig. 4D). These results indicate that silencing *SlSUT4* enhanced sucrose efflux from source leaves and thus increased soluble sugar accumulation in the shoot apex.

Silencing *SlSUT4* promotes SlSUT1 localization at the plasma membrane

The increase of sucrose export mediated by *SlSUT4* silencing led us to investigate the expression of other *SlSUT* family members. SlSUT1 is a major phloem loader and plays a role in long-distance sucrose transport (Hackel et al. 2006). SlSUT2 has been proposed as a putative receptor of extracellular sucrose (Barker et al. 2000). Silencing *SlSUT4* did not affect the expression of *SlSUT1* or *SlSUT2* (Supplemental Fig. S4, A and B), suggesting that the increase of sucrose export in the *SlSUT4*-RNAi lines may not be attributed to any alteration in the transcription of *SlSUT1* or *SlSUT2*. Previously, SlSUT4–SlSUT1 interaction was

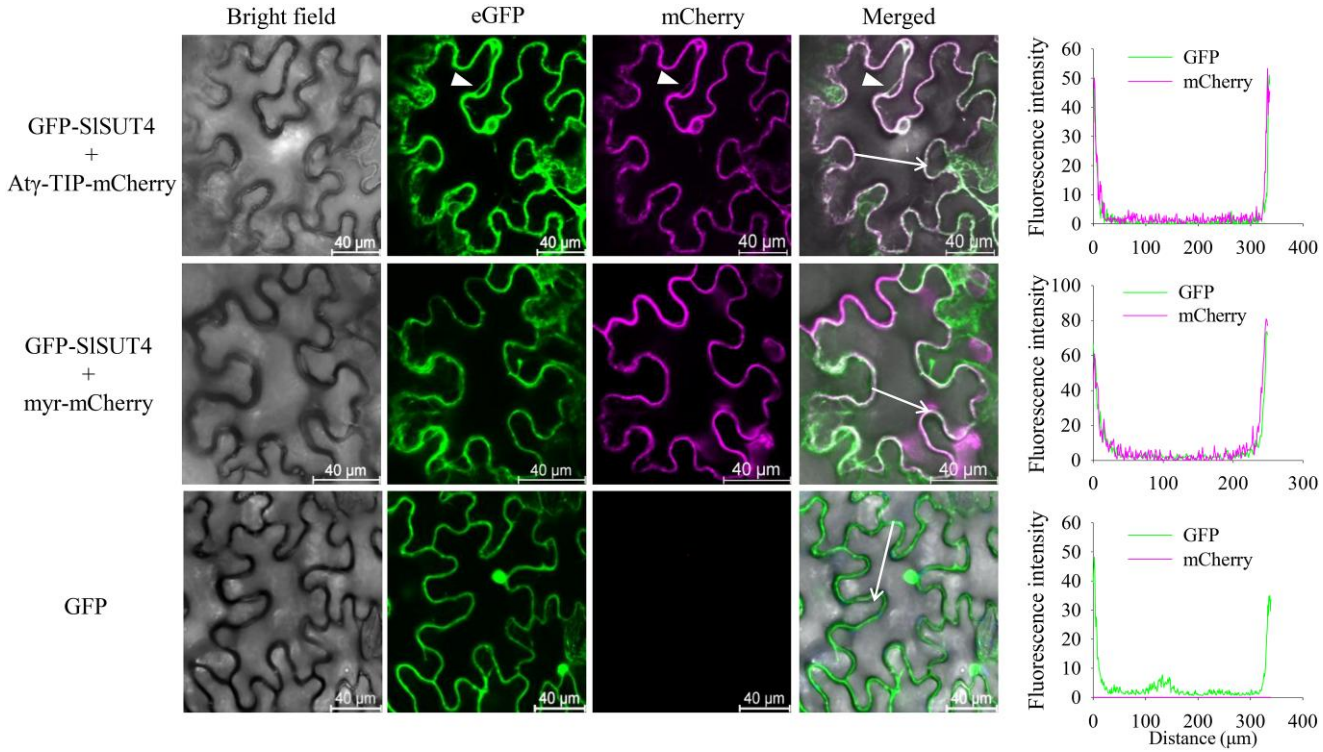

Figure 2. Subcellular localization of SlSUT4 in *N. benthamiana* leaves. The constructs carrying *Atγ-TIP-mCherry* and *myr-mCherry* were used as tonoplast- and plasma membrane-localized markers, respectively. The vector carrying *GFP* only was used as a positive control. The constructs carrying *GFP-SlSUT4* and the ones carrying *Atγ-TIP-mCherry* or *myr-mCherry* were transiently co-transformed into epidermal cells of *N. benthamiana* leaves. The fluorescence was observed under a confocal laser scanning microscope at excitation wavelengths of 488 nm for GFP and 552 nm for mCherry. mCherry is shown in magenta. The arrowheads point to transvacuolar strands. The fluorescence signal strength was analyzed with ImageJ. The white arrows indicate paths used for generating the fluorescence intensity profiles on the right.

found using the yeast split-ubiquitin system (Reinders et al. 2002). In this study, the effect of the interaction on subcellular targeting specificity of SlSUT1 was analyzed by co-expression of *GFP-SlSUT4* and *SlSUT1-mCherry* in *N. benthamiana* epidermal cells, and the western blotting result showed that the relative proportion of SlSUT1-mCherry was decreased in the plasma membrane when *SlSUT1* and *SlSUT4* were co-expressed compared with that *SlSUT1* was co-expressed with *GFP* (Fig. 5A). This result suggests that interaction of SlSUT4 and SlSUT1 decreases the targeting specificity of the latter to the plasma membrane and causes its internalization. We then analyzed SlSUT1 protein abundance in the microsomal membrane and plasma membrane in the wild-type and *SlSUT4*-RNAi plants. Our results showed that silencing *SlSUT4* did not change SlSUT1 abundance in the microsomal membrane but increased the protein abundance in the plasma membrane (Fig. 5B), which further proved that the targeting specificity of SlSUT1 to plasma membrane was regulated by its interaction with SlSUT4. These results suggest that silencing *SlSUT4* promotes SlSUT1 localization at the plasma membrane, which may have contributed to the increased sucrose export.

GA biosynthesis is suppressed by high sucrose level in the *SlSUT4*-RNAi plants

We noticed that the plant height and internode length were significantly decreased in the *SlSUT4*-RNAi plants compared with the wild type (Supplemental Fig. S5, A to C), which is similar to the low GA phenotype (Li et al. 2012). Therefore, we detected the GA concentration in the shoot apex of both plants. GA_1, GA_3, and GA_4 are major active GAs in tomato (Chen et al. 2016). Our results showed that the concentrations of GAs, especially GA_1 and GA_4, were obviously decreased in the *SlSUT4*-RNAi plants (Fig. 6A). The expression of the main GA biosynthetic genes, including *SlGA20ox1* (Solyc03g006880.1.1), *SlGA20ox3* (Solyc11g072310.1.1), *SlGA3ox1* (Solyc06g066820.4.1), and *SlKO* (Solyc04g083160.1) (Mignolli et al. 2015), was also significantly decreased in the *SlSUT4*-RNAi plants (Fig. 6, B and C). Besides, the expression of *PRO/DELLA*, which activates *FA/LFY* and *MC/AP1* to control flowering in tomato (Silva et al. 2019), was higher in the *SlSUT4*-RNAi plants than the wild type (Fig. 6D). These results imply that silencing *SlSUT4*-induced increase in shoot apex sucrose level inhibited GA biosynthesis and thus promoted tomato flowering.

To confirm the regulatory role of sucrose on flowering and GA biosynthesis, we treated the wild-type tomato seedlings

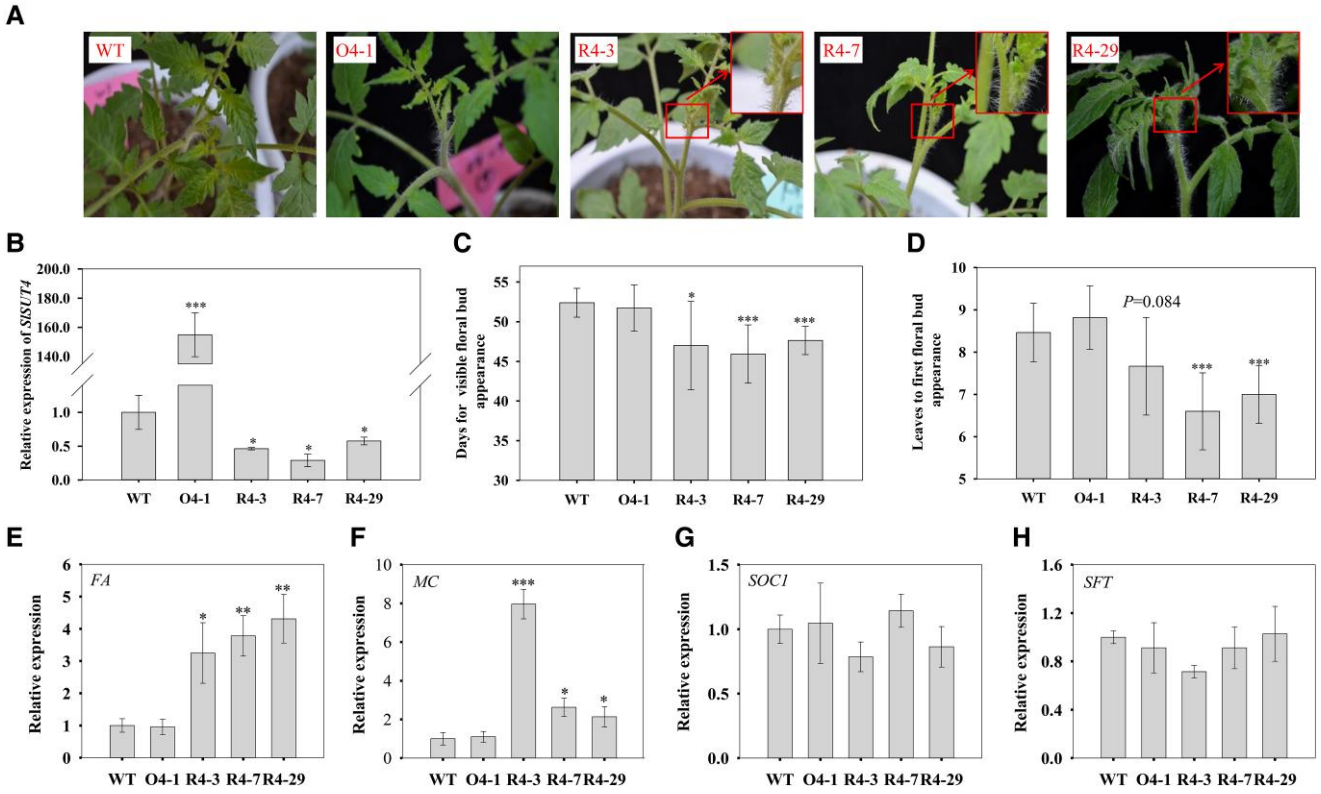

Figure 3. Effect of altered *SlSUT4* expression on tomato flowering. **A)** The early flowering phenotype of *SlSUT4*-RNAi plants. **B)** *SlSUT4* expression in the transgenic plants. **C)** Days for first floral bud appearance. **D)** Leaves to first floral bud appearance. **E** to **H)** Relative expressions of *FA* **(E)**, *MC* **(F)**, *SOC1* **(G)**, and *SFT* **(H)**. The gene expressions were analyzed using RT-qPCR, and *actin* and *ubiquitin* were used as internal controls. Data are means ± SD ($n = 3$ to 28 for flowering time analysis and 3 for gene expression analysis). The data were subjected to Student's *t*-test, and asterisks above bars indicate significant differences compared with the wild type. *$P < 0.05$, **$P < 0.01$, and ***$P < 0.001$. WT, wild type; O, overexpression line; R, RNAi line.

with exogenous sucrose and GA. The results showed that in contrast to the effect of GA, sucrose treatment decreased the plant height and promoted tomato flowering (Fig. 7, A and B). The expression of *FA/LFY* and *MC/AP1* as well as *PRO/DELLA* was decreased by GA treatment, but all increased after sucrose treatment (Fig. 7, C to E). Sucrose treatment decreased the expression of *SlGA20ox1*, *SlGA20ox3*, *SlKO*, and *SlKAO* (Solyc08g007050.2.1) (Fig. 7, F and G) and the levels of GAs, especially GA_1 and GA_4 (Fig. 7H). These results suggest that sucrose can inhibit GA biosynthesis and thus GA signaling.

A sucrose-induced R2R3 MYB transcription factor SlMYB76 directly binds to the promoters of *SlKO* and *SlGA20ox1* and represses their expression

Given that both silencing *SlSUT4* and exogenous sucrose treatment inhibited *SlGA20ox1* and *SlKO* expressions, we analyzed the promoter sequences of these two genes. The results showed that the promoters contain several MYB-binding sites (Supplemental Fig. S6). Transcriptome analysis on the wild-type and *SlSUT4*-RNAi plants demonstrated differential expressions of some MYB transcription factor genes, among which the expression of a R2R3 MYB gene *SlMYB76* was increased in the *SlSUT4*-silenced plants. Reverse transcription quantitative PCR (RT-qPCR) analysis confirmed the result (Fig. 8A). Moreover, the expression of this gene was also increased by sucrose treatment (Fig. 8B). When analyzing the promoter of *SlMYB76*, we found a potential *cis*-acting element - sucrose response element (SURE) box (Fig. 8C). To verify whether the element was functional, we conducted transient expression assay in *N. benthamiana* leaves with a GUS reporter gene driven by tandem repeats of the SURE box (Fig. 8D). The result showed that the expression of *GUS* in 4 × SURE-box infiltrated leaves was induced by exogenous sucrose, implying the involvement of this *cis*-acting element in sucrose-induced *SlMYB76* expression (Fig. 8E).

Next, we examined whether SlMYB76 could directly bind the promoters of *SlKO* and *SlGA20ox1*. Our result of yeast one-hybrid (Y1H) assay preliminarily proved the interactions (Fig. 9, A and B). Meanwhile, dual-luciferase assay showed that co-expression of *SlMYB76* inhibited the expression of the *SlKO* and *SlGA20ox1* pro-LUC reporter genes compared with the empty vector (Fig. 9, C and D). Furthermore, the electrophoretic mobility shift assay (EMSA) result also

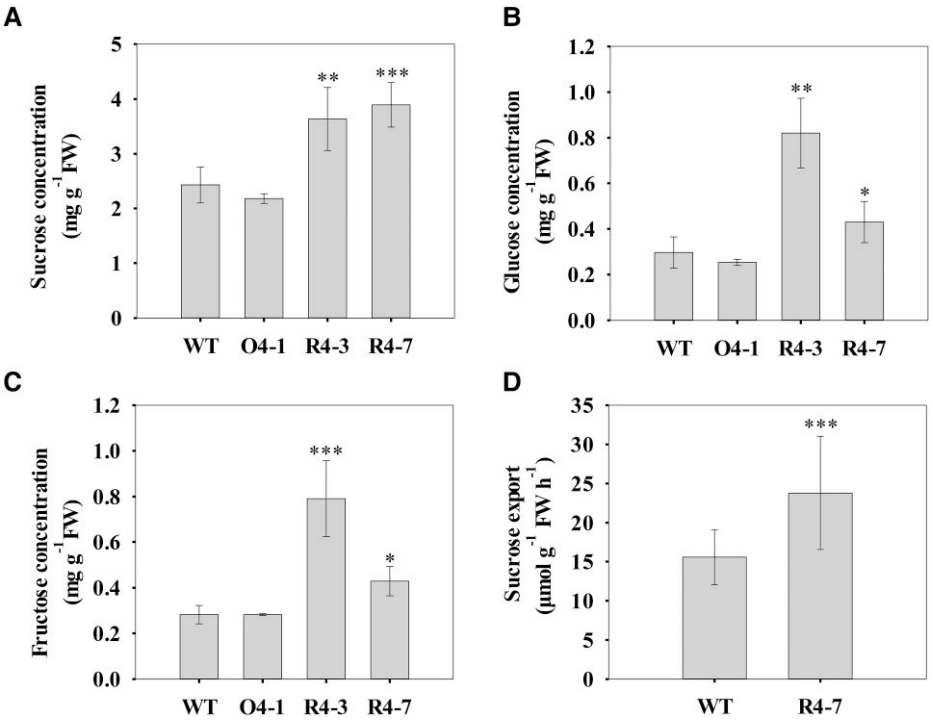

Figure 4. Effect of altered *SlSUT4* expression on the soluble sugar concentrations in the shoot apex and sucrose efflux. **A** to **C)** Concentrations of soluble sugars in shoot apex. **D)** Sucrose content of phloem exudates from detached, fully expanded tomato leaves. Exudation into 20 mM EDTA (pH 7.8) was allowed for 5 h in the dark. Data are means ± SD ($n = 3$ to 5 for shoot apex sugar concentration and 12 for sucrose export rate). The data were subjected to Student's *t*-test, and asterisks above bars indicate significant differences compared with the wild type. *$P < 0.05$, **$P < 0.01$, and ***$P < 0.001$. FW, fresh weight; WT, wild type; O, overexpression line; R, RNAi line.

demonstrated that SlMYB76 bound the promoters of *SlKO* and *SlGA20ox1* in vitro (Fig. 9, E and F). In addition, the interaction was also confirmed by chromatin immunoprecipitation qPCR (ChIP-qPCR) (Fig. 9, G and H).

To further verify the function of *SlMYB76*, we performed virus-induced gene silencing (VIGS) on tomato plants. The results showed that the VIGS-silenced plants had higher plant height (Fig. 10, A and B) and the *SlMYB76* expression was reduced by 90% (Fig. 10C), suggesting that VIGS was effective in silencing *SlMYB76* expression. The downregulation of *SlMYB76* expression significantly upregulated the *SlKO* and *SlGA20ox1* expression as well as the GA levels in the shoot apex (Fig. 10, D to F). These results indicate that sucrose-induced SlMYB76 negatively regulates GA biosynthesis through a direct binding to the promoters of *SlKO* and *SlGA20ox1* to repress their expressions.

Discussion

SlSUT4 is a functional SUT in tomato

SUTs are involved in cellular H^+-coupled sucrose transport (Williams et al. 2000). The functions of SUTs differ among the family members. The physiological function of SUT1 has been intensively studied, while that of SUT4 was less understood in many plant species including tomato. In this study, we found that the expression of *SlSUT4*, *AtSUC2*, or *AtSUT4* could rescue the invertase-deficient SUSY7/ura3 yeast cells to normal growth (Fig. 1, A and B), and SEY6210 yeast cells expressing either of these genes could take up esculin, an analog of sucrose (Fig. 1, C to H), suggesting the functionality of SlSUT4 in sucrose transport. Weise et al. (2000) previously reported that SlSUT4 was not functional in sucrose transport when expressed in yeasts, whereas we have provided convincing evidence here showing that SlSUT4 acts as a functional SUT in tomato, like AtSUC2 (Sauer and Stolz 1994) and AtSUT4 (Weise et al. 2000) in Arabidopsis. The reason for this inconsistency is unknown. Different tomato genotypes were used in the two studies - "UC82b" in Weise et al. (2000) and "M82" in this study, and there is one amino acid difference at the position of 203 - proline in "M82" and leucine in "UC82b" (Supplemental Fig. S1B). However, 3D structure prediction did not show an obvious difference in the topological structure between the two proteins (Supplemental Fig. S7). The importance of this amino acid for sucrose transport activity needs to be investigated in future.

The results for subcellular localization of SUT4-type transporters have been mixed in different plants and even in the same plant species, with most of the members being reported to possess at least two different compartments (Chincinska et al. 2013). For SlSUT4 from tomato,

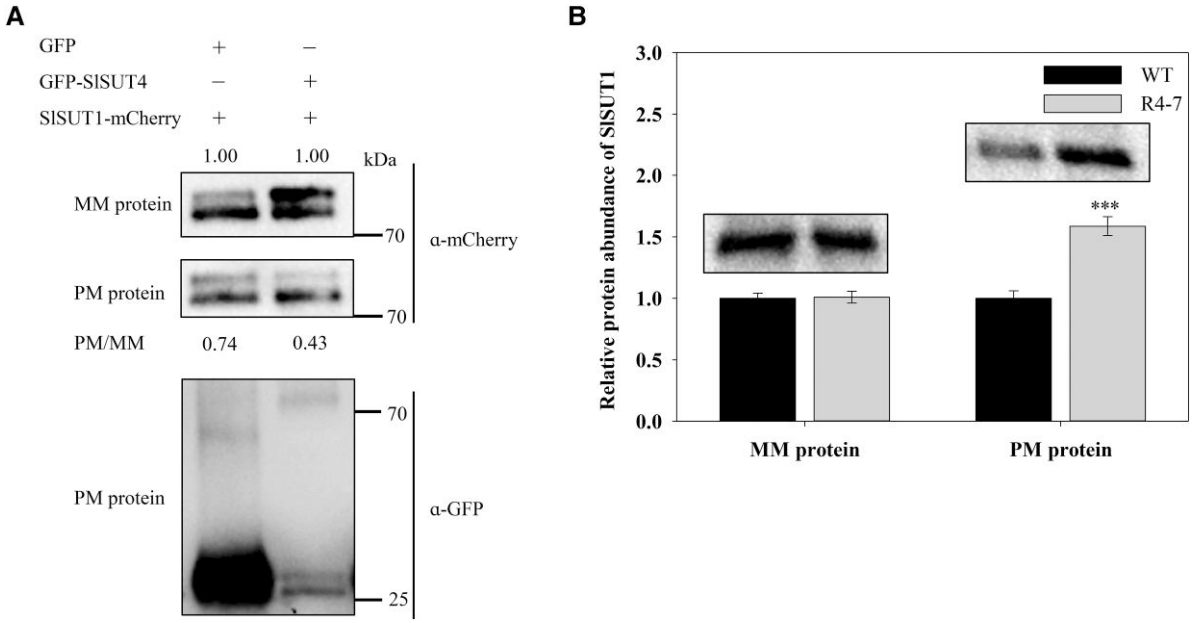

Figure 5. Internalization of SlSUT1. **A)** Partial internalization of SlSUT1 from the plasma membrane caused by co-expression of *GFP-SlSUT4* and *SlSUT1-mCherry* in *N. benthamiana* leaf cells. Ten-microgram microsomal membrane proteins and 3-μg plasma membrane proteins were separated by 10% (*w*/*v*) sodium dodecyl sulfate-polyacrylamide gel electrophoresis, and western blotting analysis on mCherry and GFP was conducted with their antibodies, respectively. The numbers (0.74 and 0.43) indicate the relative quantity of SlSUT1 in plasma membrane normalized to that in microsomal membranes. These values do not represent the relative quantity of SlSUT1 in the microsomal membrane protein. **B)** Effect of silencing *SlSUT4* on SlSUT1 protein abundance in the microsomal membrane and plasma membrane of tomato leaves. Fifty-microgram microsomal membrane proteins and 30-μg plasma membrane proteins were separated by 10% (*w*/*v*) sodium dodecyl sulfate-polyacrylamide gel electrophoresis. The SlSUT1 protein abundance was analyzed using western blotting assay with a specific antibody against SlSUT1. Data are means ± SD ($n = 3$). The data were subjected to Student's *t*-test, and asterisks above the bar indicate a significant difference compared with the wild type. ***$P < 0.001$. WT, wild type; R, RNAi line; MM, microsomal membrane; PM, plasma membrane.

Weise et al. (2000) reported its localization at the plasma membrane. Here, we observed that the fluorescence signal of SlSUT4-GFP was not as clear as that of GFP-SlSUT4. This may be due to the trapping of the former fusion protein with the secretory machinery membranes (Romsicki et al. 2004). Therefore, we used the *GFP-SlSUT4* construct for the localization. With the introduction of corresponding markers, our results confirmed that SlSUT4 was localized at both plasma membrane and tonoplast (Fig. 2). The plasma membrane localization of SlSUT4 was also supported by the data from the sucrose transport experiments in yeasts (Fig. 1, B, E, and H), where plasma membrane localization is a prerequisite for the entry of sucrose. The importance of the dual targeting of SUT4 in tomato as well as in potato is unknown and needs to be elucidated in future.

Silencing *SlSUT4* promotes sucrose transport to the shoot apex by enhancing SlSUT1 targeting on the plasma membrane

In this study, we observed that silencing *SlSUT4* promoted tomato flowering (Fig. 3, A to D), which corresponded with the increased sucrose efflux rate from source leaves and higher levels of soluble sugars in the shoot apex (Fig. 4, A to D). These results are consistent with those observed in potato (Chincinska et al. 2008). However, the reason for the increase of sucrose transport to the shoot apex of *SUT4*-silenced plants is unknown. SUT1, which is localized at the plasma membrane, is the most critical SUT for sucrose efflux from source leaves (Chincinska et al. 2008), and its activity can be regulated at transcriptional and posttranscriptional levels. Here, transcriptional regulation of SlSUT1 by SlSUT4 is unlikely, since silencing *SlSUT4* did not affect the *SlSUT1* expression (Supplemental Fig. S5A). Protein–protein interaction and oligomerization are two of the posttranscriptional regulation modes of SUTs (Garg et al. 2020). Oligomer formation can affect the subcellular targeting of SUTs, with differential responses among individuals (Garg et al. 2020; Garg and Kühn 2022). For example, both homodimer formation and heterodimer formation of potato StSUT1 increase its internalization, whereas the homodimers of SlSUT2 or its heteromeric complex with v-SNARE/VAMP711 increase plasma membrane targeting of SlSUT2. Previously, the yeast two-hybrid technique has shown that SlSUT4 can interact with SlSUT1 (Reinders et al. 2002). It is possible that SlSUT1–SlSUT4 heterodimer can form in the cells. In this study, co-expression of *SlSUT1* and *SlSUT4* in *N. benthamiana*

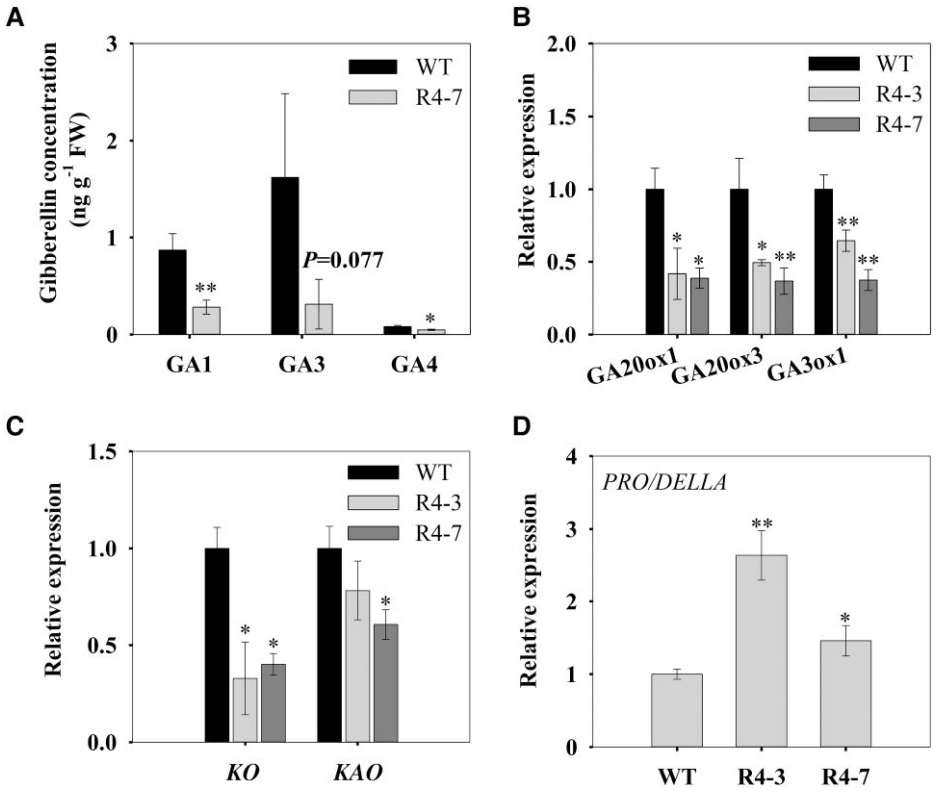

Figure 6. Effect of silencing SlSUT4 on GA synthesis and signaling. **A)** Shoot apex GA concentration. **B, C)** Expression of GA biosynthetic genes. **D)** Expression of *PRO/DELLA*—a central repressor of GA signaling. The gene expression was analyzed by RT-qPCR, and *actin* and *ubiquitin* were used as internal controls. Data are means ± SD ($n = 3$). The data were subjected to Student's *t*-test, and asterisks above bars indicate significant differences compared with the wild type. *$P < 0.05$ and **$P < 0.01$. WT, wild type; R, RNAi line; GA, gibberellin; FW, fresh weight.

leaves caused partial internalization of SlSUT1 from the plasma membrane (Fig. 5A), and the SlSUT1 protein proportion in the plasma membrane was increased in the *SlSUT4*-RNAi plants (Fig. 5B). These results may indicate that heterodimer formation of SlSUT1 and SlSUT4 increases internalization of SlSUT1, while in the *SlSUT4*-RNAi plants, the decreased level of SlSUT4 protein promoted SlSUT1 localizing at the plasma membrane and thus increased sucrose efflux, which contributed to the increased shoot apex sucrose level. Previous researchers have found that transgenic tobacco plants overexpressing spinach *SoSUT1* demonstrated early flowering and lack of shade avoidance response phenotypes (Liesche et al. 2011), exactly as described for StSUT4-silenced potato plants (Chincinska et al. 2008). The lack of shade avoidance response in *StSUT4*-RNAi plants seems to be due to the far-red light sensitivity of *StSUT4* mRNA stability (Liesche et al. 2011). This evidence also supports the idea that SUT4 acts as an inhibitor of SUT1. In addition, in this study, 2 SlSUT1-mCherry bands were recognized by the mCherry antibody (Fig. 5A). This could be caused by posttranscriptional regulation, such as phosphorylation modification, which can increase the molecular weight of SUT1, as has been observed in Arabidopsis SUT SUC2 (Xu et al. 2020).

Sucrose induces *SlMYB76* expression to suppress GA biosynthesis

Although sucrose has been known to induce flowering in different plants (Cho et al. 2018; Quiroz et al. 2021), the molecular mechanism is still not very clear. Garg et al. (2021) found that miR172 is involved in the flowering induction of potato plants in a sucrose-dependent manner, and it seems to be a downstream signaling component of StSUT4 in regulating flowering. Recently, Garg et al. (2022) published the protein interaction partners of StSUT4 in potato, and it is interesting to note that StSUT4 can physically interact with the ethylene receptor ETR2. Haydon et al. (2017) found that sucrose together with ethylene can regulate the protein stability of GIGANTEA, which gates GA signaling through stabilizing DELLA (Nohales and Kay 2019). Therefore, both sucrose and SUT may regulate flowering through the GA pathway. In potato, Chincinska et al. (2008) found that the expression of *GA20ox1* was decreased in the *StSUT4*-RNAi plants compared with the wild type, implying the possibility of the effect of *SUT4* expression or sucrose on GA biosynthesis. In this study, silencing *SlSUT4*-induced increase of shoot apex sucrose level (Fig. 4A) corresponded with the decreased GA level and expression of genes encoding GA biosynthesis enzymes (Fig. 6, A to C). Moreover, exogenous sucrose

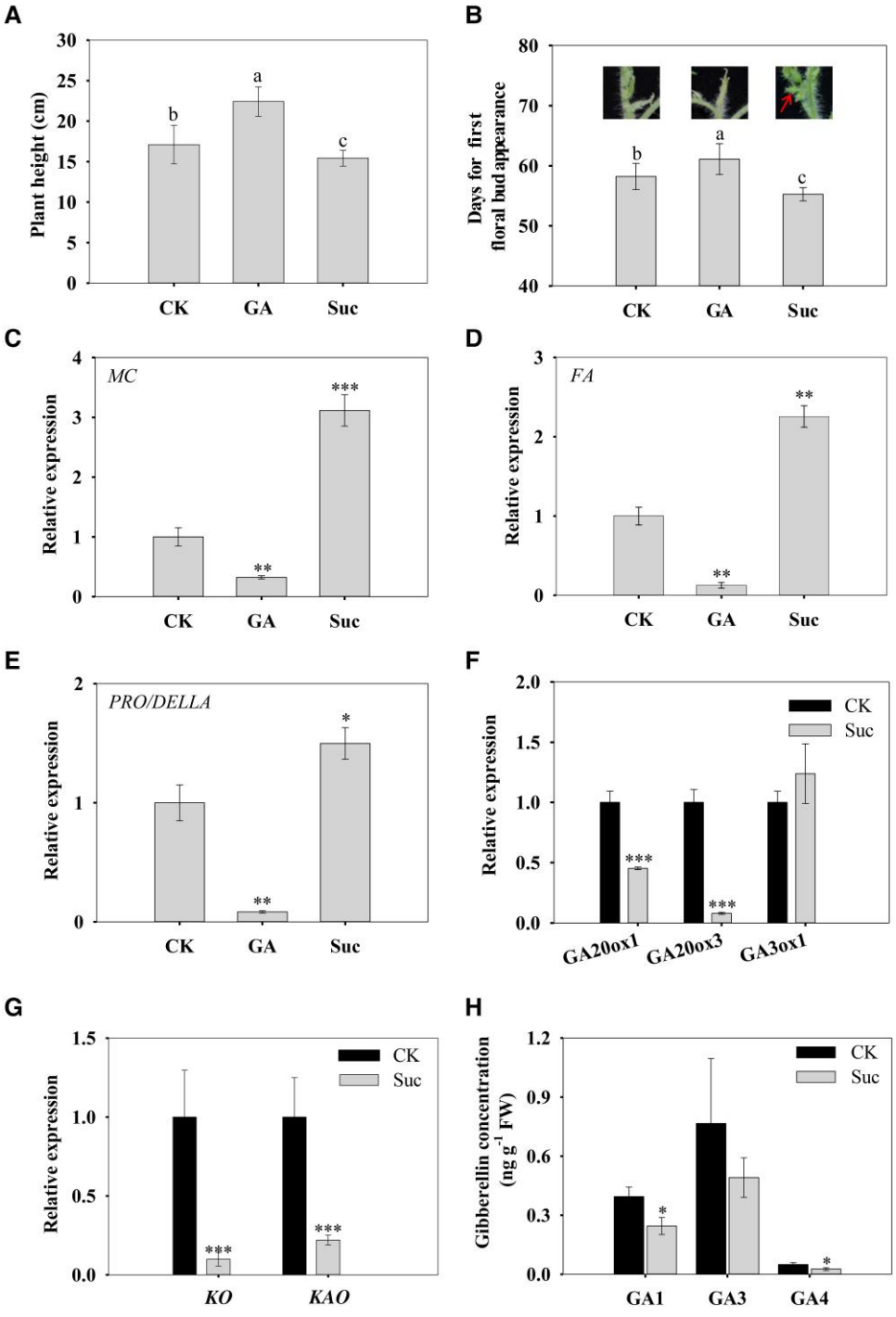

Figure 7. Effect of exogenous sucrose and GA on tomato flowering. **A)** Plant height. **B)** Days for first floral bud appearance after GA or sucrose treatment. The upper photograph shows the tomato shoot apex. **C** to **E)** Expression of *MC*, *FA*, and *PRO/DELLA* in shoot apex. The gene expression was analyzed by RT-qPCR, and *actin* and *ubiquitin* were used as internal controls. **F, G)** Expression of GA biosynthetic genes. **H)** Shoot apex GA concentration. Data are means ± SD ($n = 9$ to 11 for flowering time and plant height analysis and 3 for gene expression and GA analysis). Different letters above bars indicate significant differences between treatments at $P < 0.05$ **(A, B)**. Asterisks above bars indicate significant differences compared with the control using Student's *t*-test **(C** to **H)**. *$P < 0.05$, **$P < 0.01$, and ***$P < 0.001$. CK, control; GA, gibberellin; Suc, sucrose.

treatment experiment further confirmed the inhibitory role of sucrose on GA biosynthesis (Fig. 7, F to H). These results suggest that sucrose induced tomato flowering by inhibiting GA biosynthesis.

A new question then arises - how sucrose inhibited the GA biosynthesis? In this study, we found that the transcription factor *SlMYB76* expression was increased in the *SlSUT4*-RNAi plants and by sucrose spraying (Fig. 8, A and B).

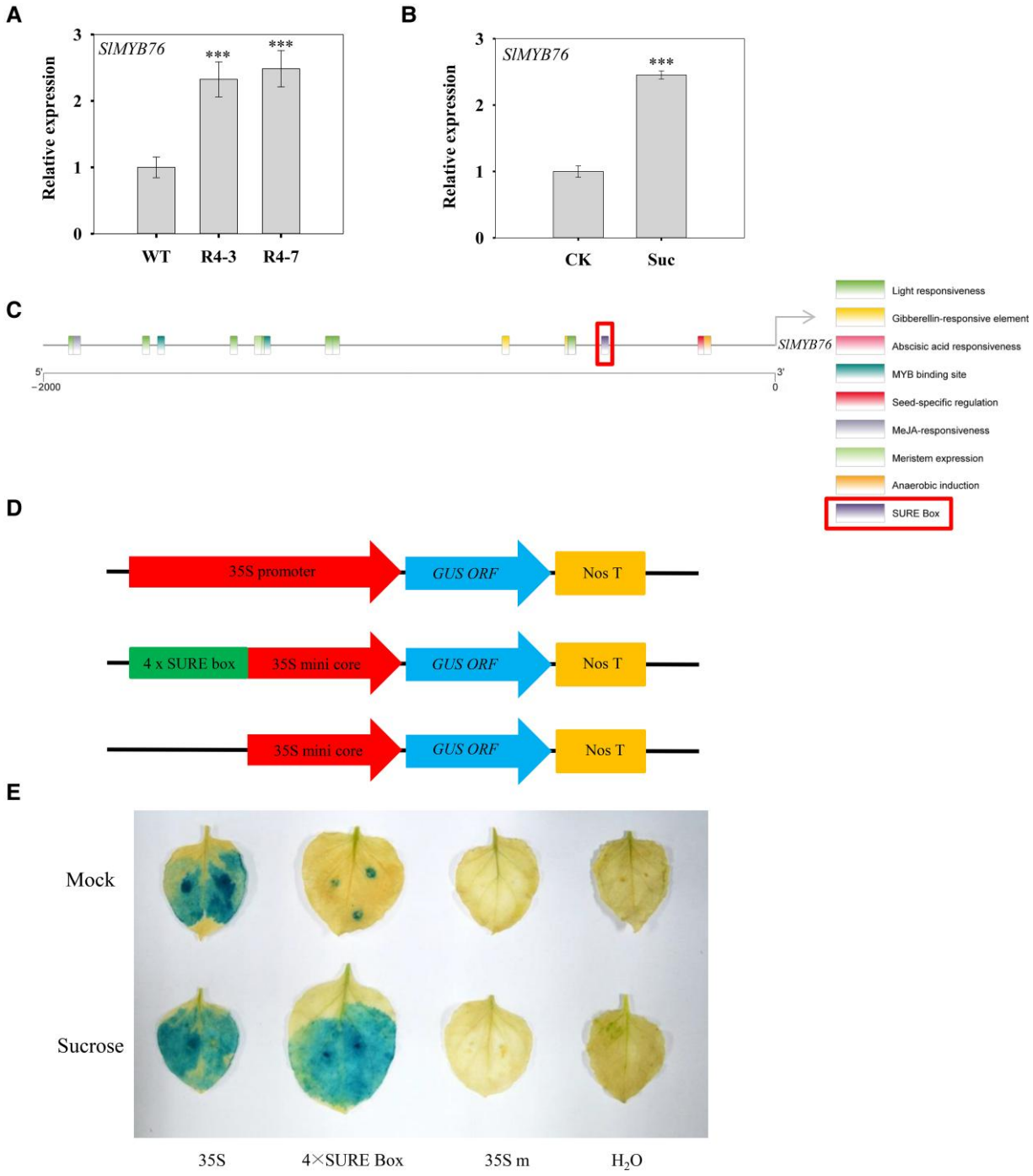

Figure 8. Expression of MYB transcription factor *SlMYB76* and response of the *cis*-acting element SURE box to sucrose. **A)** *SlMYB76* expression in *SlSUT4*-silenced plants. **B)** Effect of exogenous sucrose on *SlMYB76* expression. The gene expression was analyzed by RT-qPCR, and *actin* and *ubiquitin* were used as internal controls. Data are means ± SD ($n = 3$). The data were subjected to Student's *t*-test, and asterisks above bars indicate significant differences compared with the wild type **(A)** or control **(B)**. ***$P < 0.001$. WT, wild type; R, RNAi line; CK, control; Suc, sucrose. **C)** *Cis*-acting elements in *SlMYB76* promoter. The promoter sequence was obtained from the Solanaceae Genomics Network (https://solgenomics.net/), analyzed in PlantCARE (http://bioinformatics.psb.ugent.be/webtools/plantcare/html/), and visualized using TBtools (https://github.com/CJ-Chen/TBtools/releases). **D)** Schematic representation of vector structure used in transient *GUS* expression assay. The 46-bp core fragment of CaMV 35S promoter was used as a minimal promoter to replace the 35S promoter of pBI121 and to control the *GUS* expression as the background. **E)** Effect of SURE in *SlMYB76* promoter on *GUS* expression activity in *N. benthamiana* leaves. The 35S promoter-driven vector was used as a positive control, H_2O as a negative control, and 35S mini core-driven vector as the background. SURE, sucrose response element.

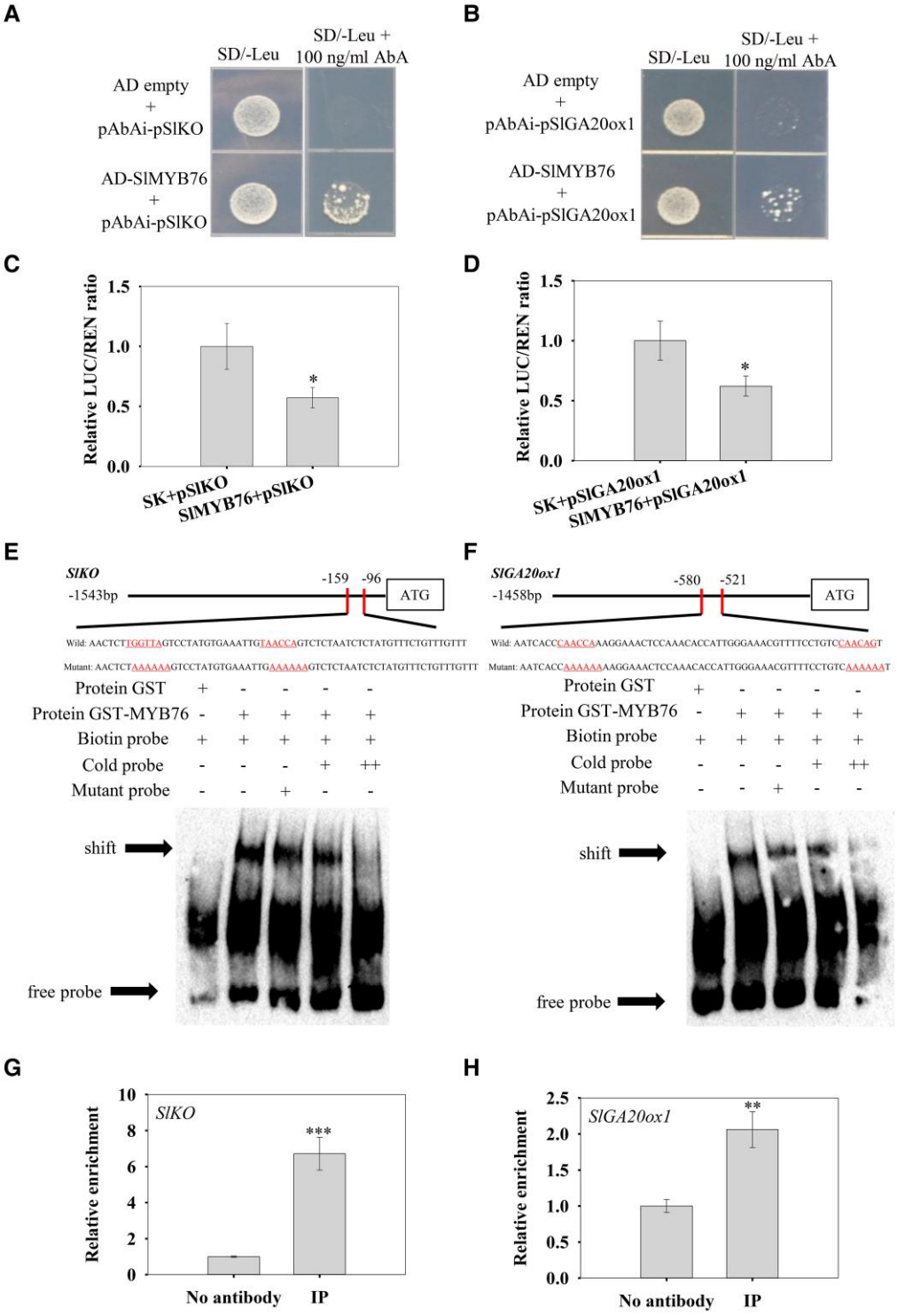

Figure 9. Verification of the interaction between SlMYB76 and the promoters of *SlKO* and *SlGA20ox1*. **A, B)** Yeast one-hybrid assay verifying the interaction between SlMYB76 and the promoters of *SlKO* **(A)** and *SlGA20ox1* **(B)**. **C, D)** Dual-luciferase assay showing that the co-expression of *SlMYB76* inhibited the expression of *SlKO* and *SlGA20ox1* pro-LUC reporter genes. The ratio of LUC to REN in the empty vector plus promoter was used as a calibrator (set as 1). The data were subjected to Student's *t*-test, and asterisks above bars indicate significant differences. $^{*}P < 0.05$. Data are means ± SD ($n = 3$). **E, F)** EMSAs showing that SlMYB76 bound to the promoter of *SlKO* and *SlGA20ox1* in vitro. The GST-SlMYB76 fusion protein was incubated with biotin-labeled probe, cold probe, and mutant probe, respectively. The GST protein incubated with biotin-labeled probe served as a negative control. − indicates absence. + indicates presence. ++ indicates increasing amounts of unlabeled probes for competition. The shifted bands are indicated by arrows. **G, H)** ChIP-qPCR analysis of SlMYB76 binding to the promoter of *SlKO* and *SlGA20ox1*. No antibody served as negative controls. Data are means ± SD ($n = 3$). The data were subjected to Student's *t*-test, and asterisks above bars indicate significant differences compared with the control. $^{**}P < 0.01$ and $^{***}P < 0.001$.

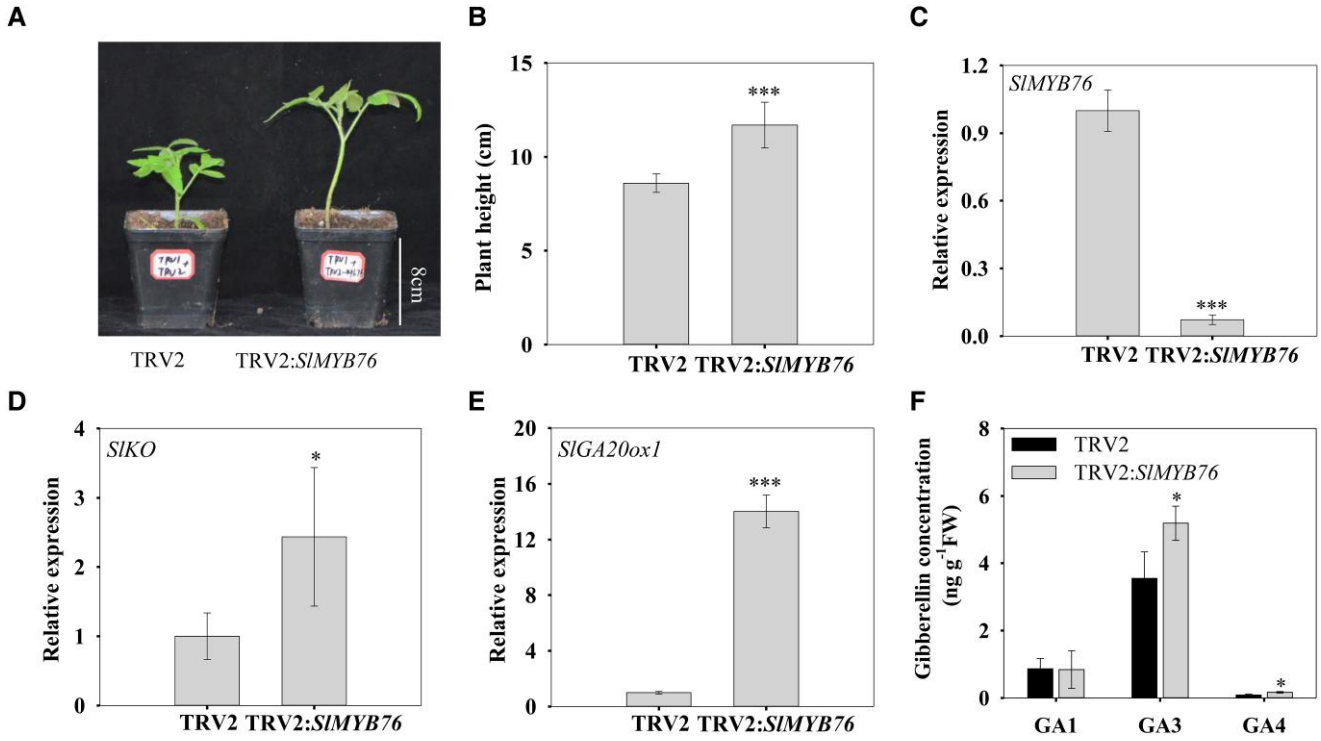

Figure 10. Effect of transient silencing *SlMYB76* on GA biosynthesis in tomato. **A)** Plant growth phenotype. **B)** Plant height. **C** to **E)** Expression of *SlMYB76*, *SlKO*, and *SlGA20ox1*. The gene expression was analyzed by RT-qPCR, and *actin* and *ubiquitin* were used as internal controls. **F)** Shoot apex GA concentration. Data are means ± SD [$n = 5$ to 7 for plant height **(B)** and 3 for gene expression and GA analysis **(C** to **F)**]. The data were subjected to Student's *t*-test, and asterisks above bars indicate significant differences compared with the control (empty vector). *$P < 0.05$ and ***$P < 0.001$. FW, fresh weight.

Promoter analysis on *SlMYB76* showed that it has a SURE box (Fig. 8C), and *GUS* expression driven by this element demonstrated its responsiveness to sucrose (Fig. 8, D and E). Moreover, SlMYB76 negatively regulated the expressions of *SlKO* and *SlGA20ox1* (Fig. 9, C and D), which encode the key enzymes in GA biosynthesis, by directly binding to their promoters (Fig. 9, A to H). The regulatory role of SlMYB76 on GA biosynthesis was further confirmed in the *SlMYB76*-silenced plants (Fig. 10, A to F). These results indicate that sucrose inhibited GA biosynthesis by inducing the expression of SlMYB76, a negative regulator of the expression of GA biosynthesis enzyme genes.

Up to date, family members of some types of transcription factors that regulate GA metabolism have been identified, such as OFP (Wang et al. 2007), DAG (Gabriele et al. 2010), KNOX, MADS-box, bHLH, TCP, and IDD/GAF (Hedden 2020). In tomato, several relevant transcription factors have also been identified. Li et al. (2012) reported that SlDREB binds to the promoter of *SlCPS* to repress its expression and thus downregulates GA biosynthesis. Chen et al. (2020) observed that SlbHLH95 represses the expression of *SlGA20ox2* and *SlKS5* by binding to their promoters. Wang et al. (2019) found that SlHY5 binds to the promoter of GA inactivation enzyme gene *SlGA2ox4*. Recently, Su et al. (2022) reported that SlBES1.8 targets the promoters of two GA inactivation enzyme genes, *SlGA2ox2* and *SlGA2ox6*. In Arabidopsis, Qi et al. (2021) found that AtMYB62 can also bind to the promoter of GA inactivation enzyme gene *AtGA2ox7*. However, few reports are available on the regulation of MYB transcription factor on GA biosynthesis genes. In this study, we demonstrated that SlMYB76 directly targeted the promoters of *SlGA20ox1* and *SlKO*, which will help us understand the regulatory mechanism of GA biosynthesis.

In conclusion, SlSUT4 is a functional SUT at the plasma membrane and tonoplast in tomato. Downregulation of *SlSUT4* expression enhances sucrose transport to the shoot apex, which promotes tomato flowering. Sucrose-induced early flowering is attributed to the repression of GA biosynthesis. This study will help us understand the function of *SlSUT4* and the molecular mechanism of sucrose in promoting flowering.

Materials and methods

Cloning of *SlSUT4*

Preparation of 3-leaf tomato (*S. lycopersicum* cv. M82) plants, and leaf RNA extraction and cDNA synthesis were as described in Jia et al. (2020). To obtain the CDS of *SlSUT4*, a pair of primers was designed (Supplemental Table S1) based on the CDS in tomato reference genome database (Solyc04g076960.2.1). PCR was performed with Primerstar

max polymerase (Takara, Kusatsu, Japan). A product of 1503 bp was obtained, cloned into pGEM-T Easy vector (Promega, Madison, WI) and sequenced by Sangon Biotech (Shanghai, China). The nucleotide acid and protein sequences of *SlSUT4* from different genotypes were aligned with DNA_{MAN} v.6 (Lynnon Biosoft, CA, USA).

Transport activity of SlSUT4

The CDS of *SlSUT4*, *AtSUC2*, and *AtSUT4* was respectively cloned into vector pDR196 at the *Sma*I and *Eco*RI sites. The primers used were listed in Supplemental Table S1. Drop test assay of yeast SUSY7/ura3 mutant was performed according to Wang et al. (2020). Uptake experiment of esculin (a sucrose analog, Wang et al. 2020) by SEY6210 yeast (*S. cerevisiae*) strain was performed according to Gora et al. (2012) and Garg et al. (2022). The esculin fluorescence was quantified on a Tecan Infinite M200pro full-wavelength multifunctional enzyme labeling instrument (TECAN, Hombrechtikon, Switzerland) with excitation and emission wavelengths of 367 and 454 nm, respectively.

Subcellular localization of SlSUT4

The CDS of *SlSUT4* without stop codon was cloned into pART27-GFP at the *Xho*I and *Hin*dIII sites to generate *SlSUT4-GFP* construct and at the *Eco*RI and *Kpn*I sites to generate *GFP-SlSUT4* construct. The CDS of γ-tonoplast intrinsic protein (TIP; AT2G36830) without stop codon was amplified from Arabidopsis (*A. thaliana*) "Col-0" and cloned into pCAMBIA1301-*mCherry* at the *Xba*I and *Kpn*I sites to generate *Atγ-TIP-mCherry* construct as a tonoplast marker (Saito et al. 2002). The myr-mCherry (a myristoylation site fused to the N-terminus of mCherry) was used as a plasma membrane marker (Du et al. 2021). The primers used were listed in Supplemental Table S1. The plasmids were transferred into *Agrobacterium tumefaciens* GV3101 using the freeze–thaw method (Dityatkin et al. 1972). Transient transformation in epidermal cells of *N. benthamiana* leaves was performed according to Champouret et al. (2009). The fluorescence was observed under a confocal laser scanning microscope (LEICA TCS SP8, Germany) with a 40×/1.4 water immersion objective. GFP excitation was performed using a 488-nm solid-state laser, and the intensity and gain were 4.9% and 800, respectively. The GFP fluorescence was detected at 498 to 540 nm. mCherry excitation was performed using a 552-nm solid-state laser, and the intensity and gain were 5% and 800, respectively. The mCherry fluorescence was detected at 590 to 640 nm. The images were postprocessed using the Leica LAS X software (Version 3.7.2). The fluorescence signal strength was generated by analyzing the gray value using ImageJ software.

Generation of *SlSUT4*-overexpressing and -RNAi transgenic tomato lines, growth phenotype and gene expression

The CDS of *SlSUT4* was amplified from tomato "M82" and cloned into pMBP-1 at the *Bam*HI and *Kpn*I sites to construct the overexpression vector. *SlSUT4*-RNAi plasmid was constructed according to Song et al. (2013). The primers used were listed in Supplemental Table S1. The constructs were transferred into *A. tumefaciens* GV3101 as described above. Tomato genetic transformation was conducted following the method of Park et al. (2003), except that 2 mg L^{-1} zeatin was added in the preculture medium instead of 6-benzyl-aminopurine and α-naphthalene acetic acid. The transgenic plants were genotyped by PCR for examining the presence of vector with specific primers (Supplemental Table S1), and the PCR products were sequenced by Sangon Biotech (Shanghai, China). The transgenic plants were grown in a greenhouse of Northwest A&F University to harvest seeds.

The 3-leaf plants of T2 generation transgenic lines and wild type were prepared according to Jia et al. (2020), and they were then transplanted in pots filled with a mixed substrate (peat:vermiculite:perlite = 2:1:1; Tianfeng, Shandong, China). When the first floral bud appeared, the days from germination and leaf number were recorded. The second fully expanded leaves (from the top) were harvested at 10:00 AM, 3:00 PM, and 9:00 PM, and shoot apexes were collected at 9:00 PM on the 45-d-old seedlings. The expressions of *SlSUT4* and flowering-related genes were analyzed by RT-qPCR. The RNA extraction and the first strand cDNA synthesis were performed according to Jia et al. (2020). The RT-qPCR was conducted using ChamQ SYBR qPCR Master Mix (711-1, Vazyme, Nanjing, China) with specific primers (Supplemental Table S2) on a QuantStudio 5 Real-Time PCR System (ABI, Carlsbad, CA). *Actin* (Solyc03g078400.3.1) and *ubiquitin* (Solyc01g068045.1.1) were used as internal controls (Sang et al. 2017). The gene expression was calculated using the $2^{-\Delta\Delta Ct}$ method (Pfaffl 2001). The plant height and the second internode length (from the bottom) were measured on the 64-d-old seedlings.

Measurement of sugar concentration and sucrose export

Soluble sugars in the leaves and shoot apex were extracted according to Xu et al. (2018) and determined with an ion chromatograph equipped with integrated pulse amperometric detector (ICS-5000+, Thermo Fisher, CA, USA). CarboPac PA1 chromatographic column (4 × 250 mm i.d., 10 μm) was used as the separation column, and 2 M NaOH was used as the mobile phase at 1 ml min^{-1}. The soluble sugar concentrations were calculated by the peak area normalizing method using Chromeleon 7 software (Thermo Fisher, CA, USA). The residue left after soluble sugar extraction was used for starch extraction and determination according to Lin et al. (1988). The export rate of sucrose was analyzed using the EDTA-facilitated exudation method (Xu et al. 2018).

Co-expression of *SlSUT1* and *SlSUT4* in *N. benthamiana* leaves and western blotting analysis

The CDS of *SlSUT1* without stop codon was cloned into pART27-*mCherry* at the *Xho*I and *Hin*dIII sites to generate

SlSUT1-mCherry construct. The primers used were listed in Supplemental Table S1. This vector and the *GFP-SlSUT4* vector constructed for the subcellular localization were transferred into *A. tumefaciens* GV3101 individually, and transient expression in *N. benthamiana* leaf epidermal cells was performed according to Champouret et al. (2009).

The infiltrated *N. benthamiana* leaves were harvested for membrane protein extraction and western blotting analysis. Microsomal membrane and plasma membrane proteins were prepared using isolation kits (BB-3152 and BB-3155; BestBio, Shanghai, China). Ten-microgram microsomal membrane proteins and 3-μg plasma membrane proteins were separated by 10% (w/v) sodium dodecyl sulfate-polyacrylamide gel, and western blotting analysis on mCherry and GFP was followed the procedures of Du et al. (2021). The specific anti-GFP antibody (ABclonal, Wuhan, China) or anti-mCherry antibody (Proteintech, Wuhan, China) was added into the blocking buffer at 1:2,000 dilution, and the secondary antibody (HRP-conjugated goat anti-rabbit IgG antibody, HS101-01, TransGen, Beijing, China) was diluted at 1:5,000. The protein bands were detected using an Immobilon western blotting kit (Millipore, MA, USA) and visualized on ChemiDoc MP (Bio-Rad, CA, USA). The band of SlSUT1-mCherry protein was quantified with the ImageJ software.

Analysis of SlSUT1 protein abundance in wild-type and *SlSUT4*-RNAi plants

Five-leaf-old wild-type and *SlSUT4*-RNAi plants were harvested for membrane protein extraction. Microsomal membrane and plasma membrane proteins were extracted according to Gupta et al. (2020). Fifty-microgram microsomal membrane proteins and 30-μg plasma membrane proteins were separated by 10% (w/v) sodium dodecyl sulfate-polyacrylamide gel, and the SlSUT1 protein abundance was analyzed using western blotting assay with a specific antibody against SlSUT1 (Hackel et al. 2006; Xu et al. 2018).

GA concentration analysis

GAs in the shoot apex tissue were extracted following the method of Cong et al. (2020), and the concentrations were determined by HPLC–MS/MS (AB SCIEX Triple TOF 5600+, MA, USA).

Exogenous GA and sucrose treatment

At-2-leaf stage, the tomato "M82" plants were applied with GA (10 μM GA_3) by watering or sucrose (50 mM) by spraying the shoot apex. The treatment was applied every other day for 2 wk. The used GA and sucrose concentrations were referred to Sun et al. (2017) and Silva et al. (2019). The days taken for the first floral bud appearance were recorded, and the plant height was measured. After 6 h or 2 wk of treatments, the shoot apex was collected for analysis of gene expression and GA concentration, respectively, using the methods as described above.

Promoter analysis of *SlKO* and *SlGA20ox1*

The promoter sequences of *SlKO* and *SlGA20ox1* were obtained from the Solanaceae Genomics Network (https://solgenomics.net/), analyzed in PlantCARE (http://bioinformatics.psb.ugent.be/webtools/plantcare/html/), and visualized using TBtools (https://github.com/CJ-Chen/TBtools/releases).

Histochemical GUS activity assay

To test the response of SURE box (AAAAAATAA) in the promoter of *SlMYB76* to sucrose, the CaMV 35S promoter of pBI121 was replaced with the 35S minimal promoter fragment driven by 4×SURE box at the *Hin*dIII and *Bam*HI sites with primers listed in Supplemental Table S1. The 46-bp core fragment of 35S promoter alone was used to check the background expression of *GUS*. The plasmids were transferred into *A. tumefaciens* GV3101 and transient expression in *N. benthamiana* epidermal cells was conducted as described above. After 4 d, the infiltrated leaves were incubated in 6% (w/v) sucrose or water for 16 h, followed by an incubation in GUS reaction buffer (1 mM 5-bromo-4-chloro-3-indolyl-beta-D-glucuronide acid, 100 mM phosphate buffer, pH 7.0, 5 mM $K_3[Fe(CN)_6]$, 5 mM $K_4[Fe(CN)_6]$, and 10 mM EDTA) for 16 h at 37°C. The leaf chlorophyll was removed through rinses in a series of ethanol before being photographed.

Interaction analysis between SlMYB76 and both *SlKO* and *SlGA20ox1*

Y1H assay was performed according to the protocol for the Matchmaker Gold Yeast One Hybrid System (Clontech, CA, USA). The CDS of *SlMYB76* was cloned into pGADT7 at the *Nde*I and *Eco*RI sites to construct AD-prey vector. To construct baits, the 1,543-bp promoter fragment of *SlKO* and 1,458-bp promoter fragment of *SlGA20ox1* were respectively cloned into pAbAi at the *Kpn*I and *Xho*I sites. The primers used were listed in Supplemental Table S1. The bait plasmids were linearized and transformed into the Y1HGold yeast strain. The minimal inhibitory concentration of aureobasidin A (AbA) was screened to avoid self-activation. The AD-prey vector was transformed into the bait yeast strain, which was then grown on synthetic dextrose medium lacking leucine (SD/−Leu) with or without 100 ng ml^{-1} AbA at 30°C for 3 d and photographed.

For dual-luciferase reporter assay, the CDS of *SlMYB76* was cloned into the pGreenII 62-SK vector at the *Hin*dIII and *Bam*HI sites to act as an effector, and the promoters of *SlKO* (1,543-bp) and *SlGA20ox1* (1,458-bp) were cloned into pGreenII 0800-LUC at the *Hin*dIII and *Bam*HI sites to serve as reporter genes. The primers used were listed in Supplemental Table S1. The plasmids and pSoup helper were transferred into *A. tumefaciens* GV3101, and transient expression in *N. benthamiana* leaf epidermal cells was as described above. After 2 d, the activities of LUC and REN luciferase were measured using the Dual-Luciferase Assay Kit

(TransGen, Beijing, China) on a Tecan Infinite M200pro full-wavelength multifunctional enzyme labeling instrument (TECAN, Hombrechtikon, Switzerland).

For EMSA, the CDS of *SlMYB76* was cloned into pGEX-6P-1 at the *Sal*I and *Bam*HI sites, which contains a glutathione-S-transferase (GST) tag. The primers used were listed in Supplemental Table S1. The recombinant plasmid was transferred into the *Escherichia coli* strain BL21 (DE3) to obtain SlMYB76-GST fusion protein, which was purified using the GST-tagged protein purification kit (Beyotime, Shanghai, China). The probes were labeled with an EMSA probe biotin-labeling kit (Beyotime, Shanghai, China), and the EMSA reaction was performed using the Chemiluminescent EMSA Kit (Beyotime, Shanghai, China) according to the protocol from the manufacturer. The unlabeled probes and mutated probes were used as competitor and negative controls, respectively. The bands were detected on a ChemiDoc MP system (Bio-Rad, CA, USA).

For ChIP-qPCR analysis, about 3-g leaf samples from 35S:*SlMYB76*-GFP-expressed plants (see "Overexpression of *SlMYB76* in tomato" section) were collected and fixed in 1% (*v*/*v*) formaldehyde for 20 min under vacuum, after which they were sonicated to obtain DNA with an average length of 500 to 1,000 bp. The *SlMYB76* cross-linked DNA was purified using a ChIP Assay Kit (Beyotime, Shanghai, China). No antibody was used as a negative control, and a fragment of *actin* (Solyc03g078400.3.1) was amplified as an internal control. The enrichment of DNA regions was analyzed by quantitative real-time PCR using specific primers (Supplemental Table S2).

Overexpression of *SlMYB76* in tomato

The CDS of *SlMYB76* without stop codon was cloned into pART27-GFP at the *Xho*I and *Hind*III sites to generate *SlMYB76-GFP* construct, which was then transferred into *A. tumefaciens* GV3101. Tomato genetic transformation and genotyping were described above.

VIGS of *SlMYB76* in tomato

For VIGS of *SlMYB76* in tomato, a 300-bp CDS fragment of *SlMYB76* was inserted into pTRV2 at the *Xba*I and *Sac*I sites to generate pTRV2-*SlMYB76*. The primers used were listed in Supplemental Table S1. A fragment of *SlPDS1* (Solyc03g123760.3) was cloned into pTRV2 to generate pTRV2-*SlPDS1* as a positive control, and the empty vector served as a negative control. The VIGS experiment was performed according to Liu et al. (2002). The shoot apexes of TRV2:*SlMYB76* plants were harvested 30 d after infiltration for gene expression and GA concentration analysis. Simultaneously, the plant height was measured.

3D structure prediction of SlSUT4

The 3D structure prediction of SlSUT4 from different tomato genotypes was performed in AlphaFold2 (https://colab.research.google.com/github/sokrypton/ColabFold/blob/main/AlphaFold2.ipynb) and visualized using PyMOL software (DeLano Scientific LLC, CA, USA).

Statistical analysis

Data were subjected to one-way ANOVA using SPSS v.20 or Student's *t*-test in Excel 2010. Differences between treatments were considered to be significant at $P < 0.05$.

Accession numbers

Sequence data from this article can be found in the Solanaceae Genomics Network (https://solgenomics.net/) with the accession numbers listed in Supplemental Table S2.

Acknowledgments

We thank Prof. Yu Du from Northwest A&F University for kindly providing the pART27-*GFP*, pART27-*mCherry*, and plasma membrane marker *myr-mCherry* vectors; Prof. Zhenxian Zhang from China Agricultural University for kindly providing the vector pDR196; Prof. Peng Zhang from CAS Center for Excellence in Molecular Plant Sciences for kindly providing the yeast strain SUSY7/ura3; and Prof. Chaorong Tang from Hainan University for kindly providing the yeast strain SEY6210. We thank Yanchun Fan for the technical assistance in the determination of soluble sugars, Jing Zhao and Luqi Li for the assistance in the GA analysis, Yangyang Yuan for the assistance in the use of confocal laser scanning microscope, and Beibei He for the assistance in the use of a fluorescence microscope. We thank Prof. Johannes Liesche from the College of Life Sciences, Northwest A&F University, for kindly providing the anti-SlSUT1 antibody and giving valuable suggestions for the study. We also thank the anonymous reviewers for providing valuable suggestions to improve the manuscript.

Author contributions

H.G. and Yufei L. conceived and designed the research; Yufei L., J.B., Z.X., Z.L., J.G., and F.Z. performed the experiments; Yufei L., Yan L., H.H., and H.G. analyzed the data; Yufei L. wrote the manuscript; H.G. and H.H. revised the manuscript.

Supplemental data

The following materials are available in the online version of this article.

Supplemental Figure S1. SUT4 nucleotide acid and amino acid sequences.

Supplemental Figure S2. Subcellular localization of SUT4-GFP vs GFP-SUT4.

Supplemental Figure S3. Sucrose and starch concentrations.

Supplemental Figure S4. *SUT1* and *SUT2* expression in SUT4-RNAi plants.

Supplemental Figure S5. Phenotype of *SlSUT4*-RNAi plants.

Supplemental Figure S6. Promoters of *SlKO* and *SlGA20ox1*.

Supplemental Figure S7. 3D structure of SlSUT4.

Supplemental Table S1. Primers used for plasmid construction and transgenic genotyping.

Supplemental Table S2. Primers used for reverse transcription quantitative PCR.

Funding

This work was supported by the National Natural Science Foundation of China (32272706).

Conflict of interest statement. The authors have no conflict of interest to declare.

References

Aoki N, Scofifield GN, Wang X-D, Patrick JW, Offfler CE, Furbank RT. Expression and localisations analysis of the wheat sucrose transporter *TaSUT1* in vegetative tissues. Planta. 2004:**219**(1):176–184. https://doi.org/10.1007/s00425-004-1232-7

Bao S, Hua C, Shen L, Yu H. New insights into gibberellin signaling in regulating flowering in Arabidopsis. J Integr Plant Biol. 2020:**62**(1):118–131. https://doi.org/10.1111/jipb.12892

Barker L, Kühn C, Weise A, Schulz A, Gebhardt C, Hirner B, Hellmann H, Schulze W, Ward JM, Frommer W. SUT2, a putative sucrose sensor in sieve elements. Plant Cell. 2000:**12**(7):1153–1164. https://doi.org/10.1105/tpc.12.7.1153

Bitterlich M, Krugel U, Boldt-Burisch K, Franken P, Kühn C. The sucrose transporter SlSUT2 from tomato interacts with brassinosteroid functioning and affects *arbuscular mycorrhiza* formation. Plant J. 2014:**78**(5):877–889. https://doi.org/10.1111/tpj.12515

Champouret N, Bouwmeester K, Rietman H, van der Lee T, Maliepaard C, Heupink A, van de Vondervoort PJ, Jacobsen E, Visser RG, van der Vossen EA, et al. *Phytophthora infestans* isolates lacking class I *ipiO* variants are virulent on *Rpi-blb1* potato. Mol Plant Microbe Interact. 2009:**22**(12):1535–1545. https://doi.org/10.1094/MPMI-22-12-1535

Chen L-Q, Qu X-Q, Hou B-H, Sosso D, Osorio S, Fernie AR, Frommer WB. Sucrose efflux mediated by SWEET proteins as a key step for phloem transport. Science. 2012:**335**(6065):207–211. https://doi.org/10.1126/science.1213351

Chen Y, Su D, Li J, Ying S, Deng H, He X, Zhu Y, Li Y, Chen Y, Pirrello J, et al. Overexpression of bHLH95, a basic helix-loop-helix transcription factor family member, impacts trichome formation via regulating gibberellin biosynthesis in tomato. J Exp Bot. 2020:**71**(12):3450–3462. https://doi.org/10.1093/jxb/eraa114

Chen S, Wang X, Zhang L, Lin S, Liu D, Wang Q, Cai S, El-Tanbouly R, Gan L, Wu H, et al. Identification and characterization of tomato gibberellin 2-oxidases (GA2oxs) and effects of fruit-specific *SlGA2ox1* overexpression on fruit and seed growth and development. Hortic Res. 2016:**3**(1):16059. https://doi.org/10.1038/hortres.2016.59

Chincinska I, Gier K, Krügel U, Liesche J, He H, Grimm B, Harren FJ, Cristescu SM, Kühn C. Photoperiodic regulation of the sucrose transporter StSUT4 affects the expression of circadian-regulated genes and ethylene production. Front Plant Sci. 2013:**4**:26. https://doi.org/10.3389/fpls.2013.00026

Chincinska IA, Liesche J, Krügel U, Michalska J, Geigenberger P, Grimm B, Kühn C. Sucrose transporter StSUT4 from potato affects flowering, tuberization, and shade avoidance response. Plant Physiol. 2008:**146**(2):515–528. https://doi.org/10.1104/pp.107.112334

Cho LH, Pasriga R, Yoon J, Jeon JS, An G. Roles of sugars in controlling flowering time. J Plant Biol. 2018:**61**(3):121–130. https://doi.org/10.1007/s12374-018-0081-z

Cong L, Wu T, Liu H, Wang H, Zhang H, Zhao G, Wen Y, Shi Q, Xu L, Wang Z. CPPU may induce gibberellin-independent parthenocarpy associated with *PbRR9* in 'Dangshansu' pear. Hortic Res. 2020:**7**(1):68. https://doi.org/10.1038/s41438-020-0285-5

Ding X, Zeng J, Huang L, Li X, Song S, Pei Y. Senescence-induced expression of *ZmSUT1* in cotton delays leaf senescence while the seed coat-specific expression increases yield. Plant Cell Rep. 2019:**38**(8):991–1000. https://doi.org/10.1007/s00299-019-02421-1

Dityatkin SY, Lisovskaya KV, Panzhava NN, Iliashenko BN. Frozen-thawed bacteria as recipients of isolated coliphage DNA. BBA-Nucleic Acids Protein Synth. 1972:**281**(3):319–323. https://doi.org/10.1016/0005-2787(72)90444-3

Du Y, Chen X, Guo Y, Zhang X, Zhang H, Li F, Huang G, Meng Y, Shan W. *Phytophthora infestans* RXLR effector PITG20303 targets a potato MKK1 protein to suppress plant immunity. New Phytol. 2021:**229**(1):501–515. https://doi.org/10.1111/nph.16861

Friend DJC, Bodson M, Bernier G. Promotion of flowering in *Brassica campestris* L. cv Cere by sucrose. Plant Physiol. 1984:**75**(4):1085–1089. https://doi.org/10.1104/pp.75.4.1085

Fukazawa J, Ohashi Y, Takahashi R, Nakai K, Takahashi Y. DELLA Degradation by gibberellin promotes flowering via GAF1-TPR-dependent repression of floral repressors in Arabidopsis. Plant Cell. 2021:**33**(7):2258–2272. https://doi.org/10.1093/plcell/koab102

Gabriele S, Rizza A, Martone J, Circelli P, Costantino P, Vittorioso P. The Dof protein DAG1 mediates PIL5 activity on seed germination by negatively regulating GA biosynthetic gene *AtGA3ox1*. Plant J. 2010:**61**(2):312–323. https://doi.org/10.1111/j.1365-313X.2009.04055.x

García-Hurtado N, Carrera E, Ruiz-Rivero O, López-Gresa MP, Hedden P, Gong F, García-Martínez JL. The characterization of transgenic tomato overexpressing *gibberellin 20-oxidase* reveals induction of parthenocarpic fruit growth, higher yield, and alteration of the gibberellin biosynthetic pathway. J Exp Bot. 2012:**63**(16):5803–5813. https://doi.org/10.1093/jxb/ers229

Garg V, Hackel A, Kühn C. Subcellular targeting of plant sucrose transporters is affected by their oligomeric state. Plants (Basel). 2020:**9**(2):158. https://doi.org/10.3390/plants9020158

Garg V, Hackel A, Kühn C. Expression level of mature miR172 in wild type and *StSUT4*-silenced plants of *Solanum tuberosum* is sucrose-dependent. Int J Mol Sci. 2021:**22**(3):1455. https://doi.org/10.3390/ijms22031455

Garg V, Kühn C. Subcellular dynamics and protein-protein interactions of plant sucrose transporters. J Plant Physiol. 2022:**273**:153696. https://doi.org/10.1016/j.jplph.2022.153696

Garg V, Reins J, Hackel A, Kühn C. Elucidation of the interactome of the sucrose transporter StSUT4: sucrose transport is connected to ethylene and calcium signalling. J Exp Bot. 2022:**73**(22):7401–7416. https://doi.org/10.1093/jxb/erac378

Gora PJ, Reinders A, Ward JM. A novel fluorescent assay for sucrose transporters. Plant Methods. 2012:**8**(1):13. https://doi.org/10.1186/1746-4811-8-13

Gupta R, Kim Y-J, Kim ST. A protocol for the plasma membrane proteome analysis of rice leaves. Methods Mol Biol. 2020:**2139**:107–115. https://doi.org/10.1007/978-1-0716-0528-8_8

Hackel A, Schauer N, Carrari F, Fernie AR, Grimm B, Kühn C. Sucrose transporter LeSUT1 and LeSUT2 inhibition affects tomato fruit development in different ways. Plant J. 2006:**45**(2):180–192. https://doi.org/10.1111/j.1365-313X.2005.02572.x

Haydon MJ, Mielczarek O, Frank A, Roman A, Webb AAR. Sucrose and ethylene signaling interact to modulate the circadian clock. Plant Physiol. 2017:**175**(2):947–958. https://doi.org/10.1104/pp.17.00592

Hedden P. The current status of research on gibberellin biosynthesis. Plant Cell Physiol. 2020:**61**(11):1832–1849. https://doi.org/10.1093/pcp/pcaa092

Houssa P, Bernier G, Kinet J. Qualitative and quantitative analysis of carbohydrates in leaf exudate of the short-day plant, *Xanthium*

strumarium L. during floral transition. J Plant Physiol. 1991:**138**(1): 24–28. https://doi.org/10.1016/S0176-1617(11)80724-8

Izawa T. What is going on with the hormonal control of flowering in plants? Plant J. 2021:**105**(2):431–445. https://doi.org/10.1111/tpj.15036

Jia J, Liang Y, Gou T, Hu Y, Zhu Y, Huo H, Guo J, Gong H. The expression response of plasma membrane aquaporins to salt stress in tomato plants. Environ Exp Bot. 2020:**178**:104190. https://doi.org/10.1016/j.envexpbot.2020.104190

Kühn C, Grof CP. Sucrose transporters of higher plants. Curr Opin Plant Biol. 2010:**13**(3):288–298. https://doi.org/10.1016/j.pbi.2010.02.001

Li J, Sima W, Ouyang B, Wang T, Ziaf K, Luo Z, Liu L, Li H, Chen M, Huang Y, et al. Tomato *SlDREB* gene restricts leaf expansion and internode elongation by downregulating key genes for gibberellin biosynthesis. J Exp Bot. 2012:**63**(18):6407–6420. https://doi.org/10.1093/jxb/ers295

Li Y, Van den Ende W, Rolland F. Sucrose induction of anthocyanin biosynthesis is mediated by DELLA. Mol Plant. 2014:**7**(3):570–572. https://doi.org/10.1093/mp/sst161

Liesche J, Krügel U, He H, Chincinska I, Hackel A, Kühn C. Sucrose transporter regulation at the transcriptional, post-transcriptional and post-translational level. J Plant Physiol. 2011:**168**(12): 1426–1433. https://doi.org/10.1016/j.jplph.2011.02.005

Lifschitz E, Eviatar T, Rozman A, Shalit A, Goldshmidt A, Amsellem Z, Alvarez JP, Eshed Y. The tomato FT ortholog triggers systemic signals that regulate growth and flowering and substitute for diverse environmental stimuli. Proc Natl Acad Sci USA. 2006:**103**(16): 6398–6403. https://doi.org/10.1073/pnas.0601620103

Lin TP, Caspar T, Somerville C, Preiss J. Isolation and characterization of a starchless mutant of *Arabdopsis thaliana* (L.) Heynh lacking ADP glucose pyrophosphorylase activity. Plant Physiol. 1988:**86**(4): 1131–1135. https://doi.org/10.1104/pp.86.4.1131

Liu Y, Schiff M, Dinesh-Kumar SP. Virus-induced gene silencing in tomato. Plant J. 2002:**31**(6):777–786. https://doi.org/10.1046/j.1365-313X.2002.01394.x

Loreti E, Povero G, Novi G, Solfanelli C, Alpi A, Perata P. Gibberellins, jasmonate and abscisic acid modulate the sucrose-induced expression of anthocyanin biosynthetic genes in *Arabidopsis*. New Phytol. 2008:**179**(4):1004–1016. https://doi.org/10.1111/j.1469-8137.2008.02511.x

Micallef BJ, Haskins KA, Wanderveer PJ, Roh K-S, Shewmaker CK, Sharkey TD. Altered photosynthesis, flowering, and fruiting in transgenic tomato plants that have an increased capacity for sucrose synthesis. Planta. 1995:**196**(2):327–334. https://doi.org/10.1007/BF00201392

Mignolli F, Vidoz ML, Mariotti L, Lombardi L, Picciarelli P. Induction of gibberellin 20-oxidases and repression of gibberellin 2β-oxidases in unfertilized ovaries of entire tomato mutant, leads to accumulation of active gibberellins and parthenocarpic fruit formation. Plant Growth Regul. 2015:**75**(2):415–425. https://doi.org/10.1007/s10725-014-0002-1

Molinero-Rosales N, Jamilena M, Zurita S, Gómez P, Capel J, Lozano R. *FALSIFLORA*, the tomato orthologue of *FLORICAULA* and *LEAFY*, controls flowering time and floral meristem identity. Plant J. 1999: **20**(6):685–693. https://doi.org/10.1046/j.1365-313X.1999.00641.x

Muller-Rober B, Sonnewald I, Willmitzer L. Inhibition of the ADP-glucose pyrophosphorylase in transgenic potatoes leads to sugar-storing tubers and influences tuber formation and expression of tuber storage protein genes. EMBO J. 1992:**11**(4):1229–1238. https://doi.org/10.1002/j.1460-2075.1992.tb05167.x

Murase K, Hirano Y, Sun T-P, Hakoshima T. Gibberellin-induced DELLA recognition by the gibberellin receptor GID1. Nature. 2008:**456**(7221):459–463. https://doi.org/10.1038/nature07519

Nohales MA, Kay SA. GIGANTEA gates gibberellin signaling through stabilization of the DELLA proteins in *Arabidopsis*. Proc Natl Acad Sci USA. 2019:**116**(43):21893–21899. https://doi.org/10.1073/pnas.1913532116

Oner-Sieben S, Rappl C, Sauer N, Stadler R, Lohaus G. Characterization, localization, and seasonal changes of the sucrose transporter FeSUT1 in the phloem of *Fraxinus excelsior*. J Exp Bot. 2015:**66**(15):4807–4819. https://doi.org/10.1093/jxb/erv255

Park SH, Morris J, Park JE, Hirschi KD, Smith RH. Efficient and genotype-independent *Agrobacterium*-mediated tomato transformation. J Plant Physiol. 2003:**160**(10):1253–1257. https://doi.org/10.1078/0176-1617-01103

Pfaffl M. A new mathematical model for relative quantification in real-time RT-PCR. Nucleic Acids Res. 2001:**29**(9):e45. https://doi.org/10.1093/nar/29.9.e45

Pryke JA, Bernier G. Acid invertase activity in the apex of *Sinapis alba* during transition to flowering. Ann Bot. 1978:**42**(3):747–749.

Qi X, Tang W, Li W, He Z, Xu W, Fan Z, Zhou Y, Wang C, Xu Z, Chen J, et al. Arabidopsis G-protein β subunit AGB1 negatively regulates DNA binding of MYB62, a suppressor in the gibberellin pathway. Int J Mol Sci. 2021:**22**(15):8270. https://doi.org/10.3390/ijms22158270

Quiroz S, Yustis JC, Chávez-Hernández EC, Martínez T, de la Paz Sanchez M, Garay-Arroyo A, Álvarez-Buylla ER, García-Ponce B. Beyond the genetic pathways, flowering regulation complexity in *Arabidopsis thaliana*. Int J Mol Sci. 2021:**22**(11):5716. https://doi.org/10.3390/ijms22115716

Reinders A, Schulze W, Kühn C, Barker L, Schulz A, Ward JM, Frommer WB. Protein-protein interactions between sucrose transporters of different affinities colocalized in the same enucleate sieve element. Plant Cell. 2002:**14**(7):1567–1577. https://doi.org/10.1105/tpc.002428

Reinders A, Sivitz AB, Starker CG, Gantt JS, Ward JM. Functional analysis of LjSUT4, a vacuolar sucrose transporter from *Lotus japonicus*. Plant Mol Biol. 2008:**68**(3):289–299. https://doi.org/10.1007/s11103-008-9370-0

Reinders A, Sivitz AB, Ward JM. Evolution of plant sucrose uptake transporters. Front Plant Sci. 2012:**3**:22. https://doi.org/10.3389/fpls.2012.00022

Riesmeier JW, Willmitzer L, Frommer WB. Isolation and characterization of a sucrose carrier cDNA from spinach by functional expression in yeast. EMBO J. 1992:**11**(13):4705–4713. https://doi.org/10.1002/j.1460-2075.1992.tb05575.x

Riesmeier JW, Willmitzer L, Frommer WB. Evidence for an essential role of the sucrose transporter in phloem loading and assimilate partitioning. EMBO J. 1994:**13**(1):1–7. https://doi.org/10.1002/j.1460-2075.1994.tb06229.x

Romsicki Y, Reece M, Gauthier J-Y, Asante-Appiah E, Kennedy BP. Protein tYROSINE phosphatase-1B dephosphorylation of the insulin receptor occurs in a perinuclear endosome compartment in human embryonic kidney 293 cells. J Biol Chem. 2004:**279**(13):12868–12875. https://doi.org/10.1074/jbc.M309600200

Saito C, Ueda T, Abe H, Wada Y, Kuroiwa T, Hisada A, Furuya M, Nakano A. A complex and mobile structure forms a distinct subregion within the continuous vacuolar membrane in young cotyledons of *Arabidopsis*. Plant J. 2002:**29**(3):245–255. https://doi.org/10.1046/j.0960-7412.2001.01189.x

Sakr S, Wang M, Dédaldéchamp F, Perez-Garcia M-D, Ogé L, Hamama L, Atanassova R. The sugar-signaling hub: overview of regulators and interaction with the hormonal and metabolic network. Int J Mol Sci. 2018:**19**(9):2506. https://doi.org/10.3390/ijms19092506

Sang J, Wang Z, Li M, Cao J, Niu G, Xia L, Zou D, Wang F, Xu X, Han X, et al. ICG: a wiki-driven knowledgebase of internal control genes for RT-qPCR normalization. Nucleic Acids Res. 2017:**46**(D1):121–126. https://doi.org/10.1093/nar/gkx875

Sauer N, Stolz J. SUC1 and SUC2: two sucrose transporters from *Arabidopsis thaliana*; expression and characterization in baker's yeast and identification of the histidine-tagged protein. Plant J. 1994:**6**(1): 67–77. https://doi.org/10.1046/j.1365-313X.1994.6010067.x

Silva GFF, Silva EM, Correa JPO, Vicente MH, Jiang N, Notini MM, Junior AC, De Jesus FA, Castilho P, Carrera E, et al. Tomato floral induction and flower development are orchestrated by the interplay between gibberellin and two unrelated microRNA-controlled modules. New Phytol. 2019:**221**(3):1328–1344. https://doi.org/10.1111/nph.15492

Silverstone AL, Jung HS, Dill A, Kawaide H, Kamiya Y, Sun TP. Repressing a repressor: gibberellin-induced rapid reduction of the RGA protein in Arabidopsis. Plant Cell. 2001:**13**(7):1555–1566. https://doi.org/10.1105/tpc.010047

Sivitz AB, Reinders A, Ward JM. Analysis of the transport activity of barley sucrose transporter HvSUT1. Plant Cell Physiol. 2005:**46**(10):1666–1673. https://doi.org/10.1093/pcp/pci182

Sivitz AB, Reinders A, Ward JM. *Arabidopsis* sucrose transporter AtSUC1 is important for pollen germination and sucrose-induced anthocyanin accumulation. Plant Physiol. 2008:**147**(1):92–100. https://doi.org/10.1104/pp.108.118992

Slewinski TL, Meeley R, Braun DM. Sucrose transporter1 functions in phloem loading in maize leaves. J Exp Bot. 2009:**60**(3):881–892. https://doi.org/10.1093/jxb/ern335

Song G-Q, Sink KC, Walworth AE, Cook MA, Allison RF, Lang GA. Engineering cherry rootstocks with resistance to prunus necrotic ring spot virus through RNAi-mediated silencing. Plant Biotech J. 2013:**11**(6):702–708. https://doi.org/10.1111/pbi.12060

Su D, Xiang W, Liang Q, Wen L, Shi Y, Song B, Liu Y, Xian Z, Li Z. Tomato SlBES1.8 influences leaf morphologenesis by mediating gibberellin metabolism and signaling. Plant Cell Physiol. 2022:**63**(4):535–549. https://doi.org/10.1093/pcp/pcac019

Sun J, Wang H, Ren L, Chen S, Chen F, Jiang J. *CmFTL2* is involved in the photoperiod- and sucrose-mediated control of flowering time in chrysanthemum. Hortic Res. 2017:**4**(1):17001. https://doi.org/10.1038/hortres.2017.1

Teichmanová M, Mašková VP, Krekule J, Francis D, Lipavská H. The fission yeast mitotic activator cdc25 and sucrose induce early flowering synergistically in the day-neutral *Nicotiana tabacum* cv. Samsun. New Phytol. 2007:**176**(4):804–812. https://doi.org/10.1111/j.1469-8137.2007.02243.x

Wang S, Chang Y, Guo J, Chen J-G. Arabidopsis ovate family protein 1 is a transcriptional repressor that suppresses cell elongation. Plant J. 2007:**50**(5):858–872. https://doi.org/10.1111/j.1365-313X.2007.03096.x

Wang D, Liu H, Wang H, Zhang P, Shi C. A novel sucrose transporter gene IbSUT4 involves in plant growth and response to abiotic stress through the ABF-dependent ABA signaling pathway in sweetpotato. BMC Plant Biol. 2020:**20**(1):157. https://doi.org/10.1186/s12870-020-02382-8

Wang F, Zhang L, Chen X, Wu X, Xiang X, Zhou J, Xia X, Shi K, Yu J, Foyer CH, et al. SlHY5 integrates temperature, light, and hormone signaling to balance plant growth and cold tolerance. Plant Physiol. 2019:**179**(2):749–760. https://doi.org/10.1104/pp.18.01140

Weise A, Barker L, Kühn C, Lalonde S, Buschmann H, Frommer WB, Ward JM. A new subfamily of sucrose transporters, SUT4, with low affinity/high capacity localized in enucleate sieve elements of plants. Plant Cell. 2000:**12**(8):1345–1355. https://doi.org/10.1105/tpc.12.8.1345

Williams LE, Lemoine R, Sauer N. Sugar transporters in higher plants: a diversity of roles and complex regulation. Trends Plant Sci. 2000:**5**(7):283–290. https://doi.org/10.1016/S1360-1385(00)01681-2

Willige BC, Ghosh S, Nill C, Zourelidou M, Dohmann EMN, Maier A, Schwechheimer C. The DELLA domain of GA INSENSITIVE mediates the interaction with the GA INSENSITIVE DWARF1A gibberellin receptor of *Arabidopsis*. Plant Cell. 2007:**19**(4):1209–1220. https://doi.org/10.1105/tpc.107.051441

Xu Q, Chen S, Yun J, Chen S, Liesche J. Regulation of sucrose transporters and phloem loading in response to environmental cues. Plant Physiol. 2018:**176**(1):930–945. https://doi.org/10.1104/pp.17.01088

Xu Q, Yin S, Ma Y, Song M, Song Y, Mu S, Li Y, Liu X, Ren Y, Gao C, et al. Carbon export from leaves is controlled via ubiquitination and phosphorylation of sucrose transporter SUC2. Proc Natl Acad Sci USA. 2020:**117**(11):6223–6230. https://doi.org/10.1073/pnas.1912754117

Yamaguchi S. Gibberellin metabolism and its regulation. Ann Rev Plant Biol. 2008:**59**(1):225–251. https://doi.org/10.1146/annurev.arplant.59.032607.092804

Yang L, Xu M, Koo Y, He J, Poethig RS. Sugar promotes vegetative phase change in *Arabidopsis thaliana* by repressing the expression of *MIR156A* and *MIR156C*. eLife. 2013:**2**:e00260. https://doi.org/10.7554/eLife.00260

Yoon J, Cho L-H, Tun W, Jeon J-S, An G. Sucrose signaling in higher plants. Plant Sci. 2021:**302**:110703. https://doi.org/10.1016/j.plantsci.2020.110703

Zhang S, Zhang D, Fan S, Du L, Shen Y, Xing L, Li Y, Ma J, Han M. Effect of exogenous GA_3 and its inhibitor paclobutrazol on floral formation, endogenous hormones, and flowering-associated genes in 'Fuji' apple (*Malus domestica* Borkh). Plant Physiol Biochem. 2016:**107**:178–186. https://doi.org/10.1016/j.plaphy.2016.06.005